Neuroscience

Circadian regulation of endoplasmic reticulum calcium response in cultured mouse astrocytes

Reviewed Preprint
v2 • November 6, 2024
Revised by authors

Reviewed Preprint
v1 • April 5, 2024

Ji Eun Ryu, Kyu-Won Shim, Hyun Woong Roh, Minsung Park, Jae-Hyung Lee, Eun Young Kim

Neuroscience Graduate Program, Department of Biomedical Sciences, Ajou University Graduate School of Medicine, Suwon, Republic of Korea • Department of Brain Science, Ajou University School of Medicine, Suwon, Republic of Korea • Interdisciplinary Program in Bioinformatics, Seoul National University, Seoul, Republic of Korea • Department of Psychiatry, Ajou University School of Medicine, Suwon, Republic of Korea • Department of Oral Microbiology, College of Dentistry, Kyung Hee University, Seoul, Republic of Korea

eLife Assessment

This work describes a circadian regulation in the expression of HERP, a regulator of endoplasmic reticulum calcium, in primary astrocytic cultures. This work is **important** because it highlights the potential importance of circadian rhythms in astrocytes, even though making a direct comparison between these rhythms in vitro and in vivo remains challenging. The technical approaches used in this work (RNA-seq, siRNA, Ca2+ imaging) are a **solid** support for data interpretation.

https://doi.org/10.7554/eLife.96357.2.sa3

Abstract

The circadian clock, an internal time-keeping system orchestrates 24-hour rhythms in physiology and behavior by regulating rhythmic transcription in cells. Astrocytes, the most abundant glial cells, play crucial roles in central nervous system (CNS) functions, but the impact of the circadian clock on astrocyte functions remains largely unexplored. In this study, we identified 412 circadian rhythmic transcripts in cultured mouse cortical astrocytes through RNA sequencing. Gene Ontology analysis indicated that genes involved in Ca^{2+} homeostasis are under circadian control. Notably, *Herpud1* (*Herp*) exhibited robust circadian rhythmicity at both mRNA and protein levels, a rhythm disrupted in astrocytes lacking the circadian transcription factor, BMAL1. HERP regulated endoplasmic reticulum (ER) Ca^{2+} release by modulating the degradation of inositol 1,4,5-trisphosphate receptors (ITPRs). ATP-stimulated ER Ca^{2+} release varied with the circadian phase, being more pronounced at subjective night phase, likely due to the rhythmic expression of ITPR2. Correspondingly, ATP-stimulated cytosolic Ca^{2+} increases were heightened at the subjective night phase. This rhythmic ER Ca^{2+} response led to circadian phase-dependent variations in the phosphorylation of Connexin 43 (Ser368) and gap junctional communication. Given the role of gap junction channel (GJC) in propagating Ca^{2+} signals, we suggest that this circadian regulation of ER Ca^{2+} responses could affect astrocytic modulation of synaptic activity according to the time of day. Overall, our study enhances the understanding of how the

circadian clock influences astrocyte function in the CNS, shedding light on their potential role in daily variations of brain activity and health.

Introduction

The circadian clock orchestrates a range of behaviors, physiological processes, and cellular and biochemical activities in organisms with approximately 24-hour rhythms, facilitating adaptation to environmental changes (Bell-Pedersen et al., 2005). In mammals, the master clock localized in the suprachiasmatic nucleus (SCN) of the anterior hypothalamus synchronizes peripheral tissue clocks throughout the body to the light/dark cycle (Mohawk et al., 2012). The circadian clock's molecular mechanism is driven by a transcriptional translational feedback loop (TTFL). CLOCK and BMAL1 form a heterodimer that triggers expression of the repressor genes, *Period* (*Per*) and *Cryptochrome* (*Cry)*, along with other clock-controlled output genes. PER and CRY proteins then translocate to the nucleus, where they interact with CLOCK/BMAL1, halting further transcriptional activation. A secondary feedback loop involving the interplay between transcriptional activation by ROR and repression by REV-ERB finely regulates the rhythmic transcription of *Bmal1* (Takahashi, 2017). Recent studies have revealed that the circadian clock controls the rhythmic transcription of numerous genes, displaying notable tissue specificity. This characteristic underscores the time-of-day-specific functional specialization of diverse tissues (Mure et al., 2018; Zhang et al., 2014). Consequently, circadian clock-controlled genes significantly influence various physiological processes including development, metabolism, aging, and neurodegeneration (Lananna & Musiek, 2020; Reinke & Asher, 2019; Schultz & Kay, 2003).

Astrocytes, the most abundant glial cells in the CNS, play vital roles in maintaining homeostasis of extracellular fluids, ions, and neurotransmitters; proving energy substrates to neurons; regulating local blood flow; modulating neuronal activity through gliotransmission; and assisting in interstitial fluid drainage (Sofroniew & Vinters, 2010). Though not electrically excitable, astrocytes exhibit complex intracellular Ca^{2+} signaling, both spatially and temporally, within individual astrocytes and across astrocytic networks. Astrocytes express various types of Gq-coupled receptors activated by neurotransmitters such as ATP, epinephrine, glutamate, and dopamine *etc*. (Verkhratsky & Nedergaard, 2018). Activation of these Gq-coupled receptors initiates the inositol 1,4,5-trisphosphate receptor (IP_3R) signaling cascade, causing a release of Ca^{2+} from the ER that substantially increases intracellular Ca^{2+} levels (Guerra-Gomes et al., 2017; Verkhratsky & Nedergaard, 2018). Increases in intracellular Ca^{2+} in astrocytes are involved in regulating numerous afore-mentioned processes (Giaume et al., 2021; Verkhratsky & Nedergaard, 2018). Recent studies have shown that astrocyte Ca^{2+} signaling can regulate circadian rhythms and sleep patterns (Bojarskaite et al., 2020; Brancaccio et al., 2019).

Accumulating evidence underscores the importance of the circadian clock in astrocytes function. Cultured murine cortical astrocytes expressing a PER-luciferase reporter (PER::LUC) exhibit circadian oscillations and can be entrained by temperature cycle (Prolo et al., 2005) and vasoactive intestinal polypeptide (VIP), which synchronizes SCN (Marpegan et al., 2009). These findings provide strong evidence that a molecular clock operates in astrocytes. In addition, disruption of clock genes specific to astrocytes has been linked to a range of deleterious effects, including excessive astrocyte activation, disruptions in daily activity patterns, impaired learning, metabolic imbalances, and a shortened lifespan (Barca-Mayo et al., 2020; Barca-Mayo et al., 2017; Griffin et al., 2019; Lananna et al., 2018). Remarkably, these phenotypic changes closely resemble those observed in astrocytes during the progression of neurodegenerative diseases (Brandebura et al., 2023; Phatnani & Maniatis, 2015). Moreover, the rhythmic metabolic activity of astrocytes, including intracellular Ca^{2+} fluctuations and neurotransmitter release, is critical for circadian timing in the SCN (Brancaccio et al., 2017). Despite the emerging significance of circadian rhythms in astrocyte function in health and disease, our understanding of the link between the circadian clock and specific astrocytic functions is still limited.

In this study, we conducted a transcriptome analysis to investigate how the circadian clock regulates astrocyte function. Our research uncovered that *Herp (*homocysteine-inducible ER protein with ubiquitin like domain 1; *Herp*) exhibited a BMAL1-dependent rhythmic expression, peaking at subjective midday phase and reaching its nadir at subjective midnight phase. HERP was crucial for ER Ca^{2+} regulation by modulating the degradation of ITPRs. Importantly, the ATP-stimulated ER Ca^{2+} response varied according to time post synchronization, a dependence that was absent in cultured astrocytes from *Bmal1*$^{-/-}$mice. Furthermore, the pronounced release of Ca^{2+} during the subjective night phase led to robust phosphorylation of the Ser368 residue of CX43, diminishing cell-to-cell communication between astrocytes. Overall, our study demonstrates that the circadian clock orchestrates a variety of astrocytic processes including Ca^{2+} homeostasis by controlling the rhythmic transcription of genes, highlighting its pivotal role in CNS function.

Results

Defining circadian rhythmic transcripts in cultured mouse cortical astrocytes

To understand how the circadian clock regulates astrocyte physiology, we conducted a circadian transcriptome analysis of cultured mouse cortical astrocytes. Cultured astrocytes were synchronized using serum shock (SS) and harvested every 4hrs for 2 days starting at 12hrs post-SS. The time series astrocyte transcriptome was determined by RNA-seq (**Figure 1A**). Using a Gaussian mixture model, we defined expressed transcripts, choosing 0.577 transcripts per million (TPM) as the cut-off, corresponding to the 1% threshold in the distribution curve of highly expressed genes (**Figure 1-figure supplement 1A**). A total of 17,671 transcripts with the highest TPM values of the 12 time points exceeding 0.577, were considered expressed. To validate astrocyte enrichment, we compared the expression of marker genes for nervous cells. Our transcriptome data were replete with astrocyte markers but lacked markers for microglia, oligodendrocytes, neurons, and endothelial cells (**Figure 1-figure supplement 1B**).

Various methods have been used to identify periodicity in time-series data, such as Lomb-Scargle (Glynn et al., 2006), JTK_CYCLE (Hughes et al., 2010) and ARSER (Yang & Su, 2010), each with distinct advantages and limitations. MetaCycle, integrates these three methods, facilitating the evaluation of periodicity in time-series data without requiring the selection of an optimal algorithm (Wu et al., 2016). Additionally, BioCycle has been developed using a deep neural network trained with extensive synthetic and biological time series datasets (Agostinelli et al., 2016). Because MetaCycle and Biocycle identify periodic signal based on different algorithms, we applied both packages to identify periodicity in our time-series transcriptome data. BioCycle and MetaCycle analyses detected 321 and 311 periodic transcripts, respectively (FDR corrected, q-value < 0.05) (**Figure 1B**). Among these, 220 (53.4%) were detected by both methods, but many transcripts did not overlap. MetaCycle is known for its inability to detect asymmetric waveforms (Mei et al., 2020). In our analysis, genes with increasing waveforms like *Adora1* and *Mybph* were identified as rhythmic only by BioCycle, while *Plat* and *Il34* were identified as rhythmic only by MetaCycle (**Figure 1-figure supplement 1C**). Despite these discrepancies, the clear circadian rhythmic expression profiles of these genes led us to conclude that using the union of the two lists compensates for the limitations of each algorithm. Consequently, we identified a total of 412 circadian rhythmic transcripts (2.3% of all transcripts) (Supplementary file 1). The circadian oscillations of these transcripts are illustrated in the heatmap in **Figure 1-figure supplement 1D**.

Next, we compared rhythmic transcripts of astrocytes with those of 12 mouse tissues from CircaDB (Zhang et al., 2014), a database of circadian rhythmic genes (**Figure 1C**). A majority of the rhythmic transcripts in astrocytes (265 of 412, 65.3%) were not rhythmic or were rhythmic in one tissue. 14 transcripts were rhythmic in more than 10 tissues; most of these were core clock genes

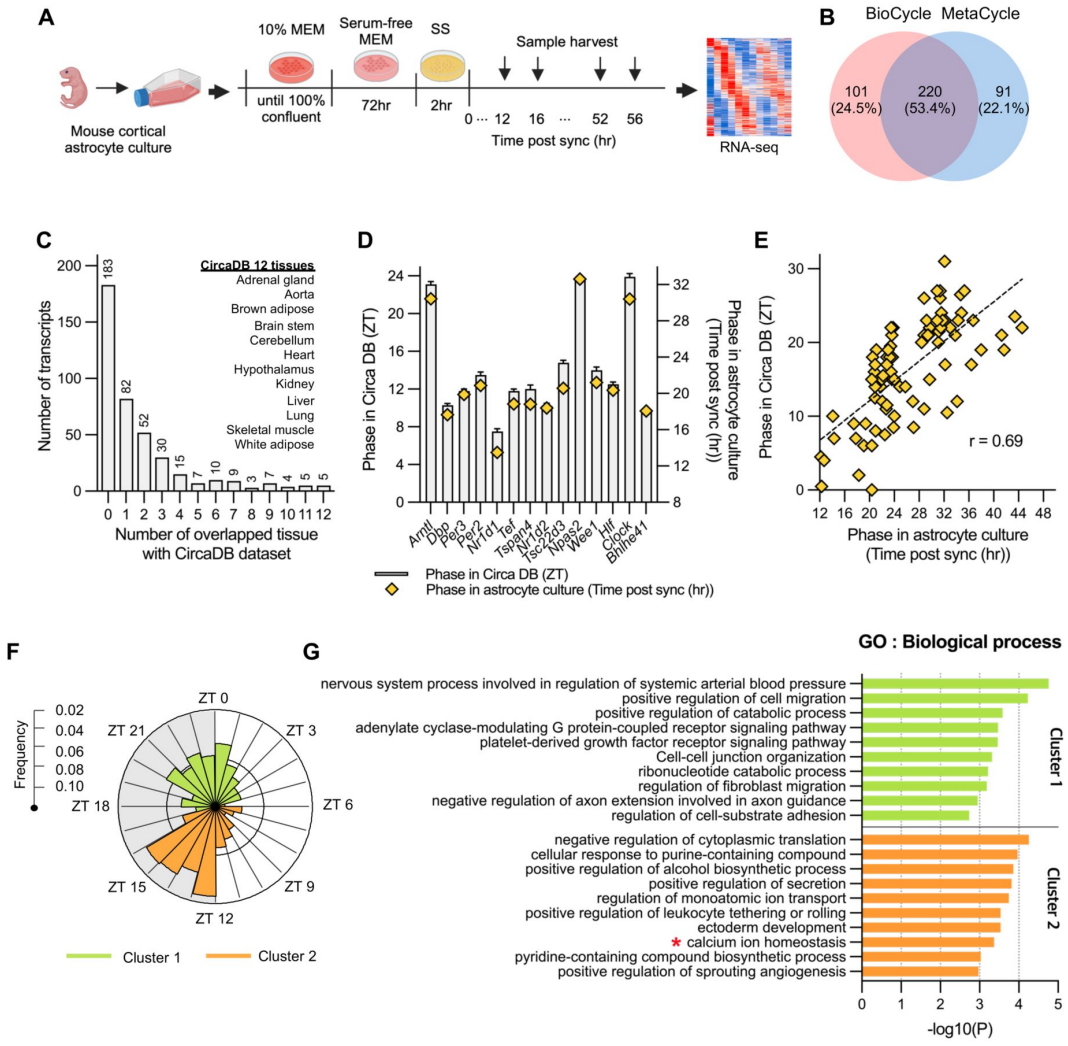

Figure 1.

Circadian rhythmic transcripts in mouse cultured cortical astrocytes.

(A) Experimental scheme for synchronizing circadian rhythms in mouse cultured cortical astrocytes followed by RNA-sequencing over 2 days. (B) Venn diagram displaying the number of circadian rhythmic transcripts identified by two algorithms ($q < 0.05$ in MetaCycle or BioCycle). (C) Number of transcripts that overlapping with 12 tissues in mouse circadian transcriptome ss from CircaDB (*http://circadb.hogeneschlab.org*). (D) Comparison of mean phase (ZT) from CircaDB and peak phase (Time post sync) from cultured astrocytes for 14 transcripts that are rhythmic in 10 or more tissues. (E) Scatter plot showing phase in CircaDB and peak phase of cultured astrocytes for transcripts that are rhythmic in one tissue. (F) Radial histogram of the distribution of phases of rhythmic genes in the astrocyte transcriptome. (G) Top 10 enriched GO Biological Process (BP) terms for significant circadian rhythmic genes in astrocytes ($p < 0.01$) identified by Metascape (*https://metascape.org*).

except *Tspan4*, *Tsc22d3*, and *Wee1*. This result is consistent with previous reports of tissue-specific circadian rhythmic expression (Mure et al., 2018; Panda et al., 2002). A phase comparison of these 14 common oscillating transcripts between CircaDB and our analysis showed a consistent time difference, with 8hrs after SS corresponding to ZT0 (**Figure 1D**). An additional phase comparison of 82 transcripts that overlapped in only one tissue indicated a very robust phase correlation between astrocytes and the corresponding tissue ($r = 0.69$, $p < 0.001$) (**Figure 1E**). Collectively, our analysis indicates that the identified oscillating transcripts were not false positive but were clearly associated with the circadian clock. Hierarchical clustering analysis of oscillating transcripts revealed two clusters: cluster 1 with 185 transcripts and cluster 2 with 227 transcripts (**Figure 1-figure supplement 2**). A circular map of peak phases across all rhythmic genes revealed two major peaks, one in the early night (ZT12 to ZT16) and one in the late night or dawn (ZT21 to ZT1) (**Figure 1F**). Here for more intuitive interpretation, we set 8hrs post synchronization (sync) to ZT0 based on a previous phase comparison. Circadian transcriptome studies conducted in multiple animal tissues have indicated that the phases of each tissue are not randomly distributed but are predominantly clustered in one or two narrow temporal windows (Panda et al., 2002). Consistent with these previous reports, mouse cultured astrocytes exhibited a high degree of temporal organization. Intriguingly, there was a relatively quiescent zone during subjective daytime, a finding different from that observed for diurnal animals, which showed a quiescent zone during subjective nighttime (Mure et al., 2018).

To understand the biological processes and pathways controlled by the circadian clock, we performed a Gene Ontology (GO) analysis on each cluster using Metascape (*https://metascape.org*) (**Figure 1G**). Given that the goal of our research was to investigate processes specifically controlled by the circadian clock, we excluded 17 core clock transcripts (*Arntl, Clock, Nfil3, Npas2, Bhlhe40, Bhlhe41, Cry1, Cry2, Dbp, Elf, Nr1d1, Nr1d2, Per1, Per2, Per3, Rorc,* and *Tef*) from our GO enrichment analysis. Among the rhythmic processes, we focused on "calcium ion homeostasis (GO:0055074)" due to the importance of intracellular Ca^{2+} signaling in numerous astrocyte functions (Agulhon et al., 2008; Bojarskaite et al., 2020; Brancaccio et al., 2019; Giaume et al., 2021; Guerra-Gomes et al., 2017; Verkhratsky & Nedergaard, 2018). In this category, Ca^{2+} homeostasis-related genes included *Herp*, *Slc4a11*, *Sord* and *Kcnh1 etc*. with *Herp* showing the most robust oscillation with large amplitude (**Table S1**).

Circadian rhythmic expression of *Herp* in cultured mouse cortical astrocytes

We first assessed the expression patterns of core clock genes and *Herp* in our cultured astrocytes. *Bmal1*, was rhythmically expressed with a peak at 30hr post sync while *Per2* and *Rev-Erbα* showed rhythmic expression with peaks at 20hr and 16hr, respectively (**Figure 2A**). *Herp* displayed a robust rhythmic expression pattern, peaking at 20hr, similar to *Per2* (**Figure 2A**). To verify the circadian expression of *Herp*, we performed quantitative real-time RT-PCR, which confirmed that *Bmal1*, *Rev-Erbα* and *Herp* exhibited circadian rhythms consistent with the RNAseq results (**Figure 2B**).

Next, we examined whether HERP protein levels also showed rhythmic changes, as many genes exhibit rhythmic transcription without corresponding protein level changes (Reddy et al., 2006). We validated the specificity of HERP antiserum using Western blot analysis of astrocytes treated with *Herp* siRNA (*Herp*-KD), which significantly reduced *Herp* mRNA levels (**Figure 2C**) and the intensities of specific bands in Western blots (**Figure 2D** and **2E**). SS-synchronized cultured astrocytes were sampled every 6hrs for 2 days and processed for Western blot analysis of BMAL1 and HERP. BMAL1 phosphorylation showed circadian variation, with hyper-phosphorylation peaking at midday and hypo-phosphorylation peaking early in the day or late at night (Yoshitane et al., 2009). In our SS-synchronized cultured astrocytes, BMAL1 was hyperphosphorylated at 18hr, 24hr, 42hr, and 48hr (corresponding to midday) and hypo-phosphorylated at 12hr, 36hr (corresponding to early in the day), and 30hr, 54hr (corresponding to late at night) throughout two

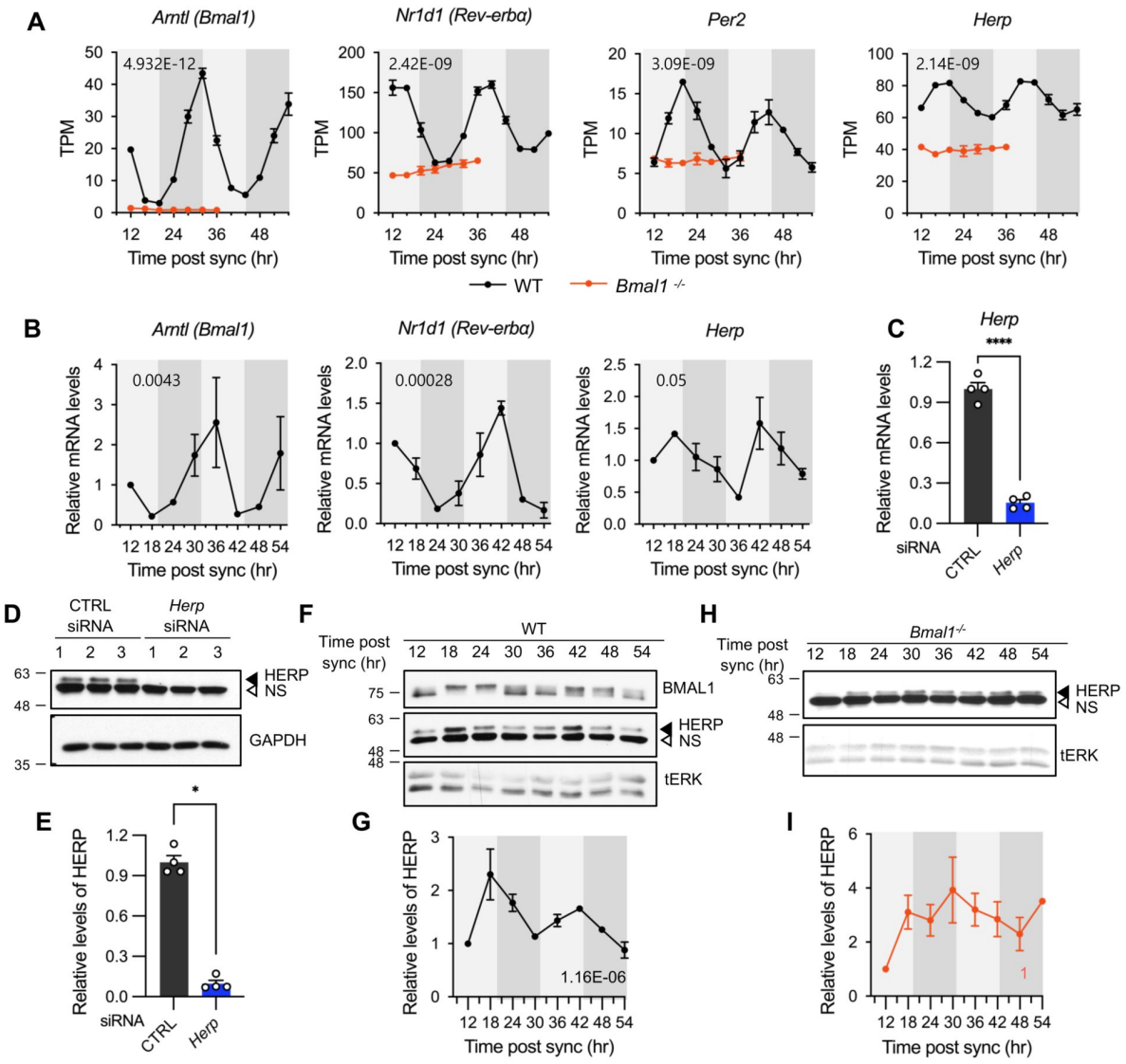

Figure 2.

Herp is rhythmically expressed in mouse cultured astrocytes and its expression is controlled by BMAL1.

(A, B) Astrocyte cultures from rom WT (black) and *Bmal1*$^{-/-}$(orange) mice were synchronized and harvested at the indicated time. Expression was analyzed for rhythmicity using MetaCycle, and expression levels of given genes were quantified using RNA-seq (A) and real-time qRT-PCR (B) data. Values are mean ± SEM (n = 2; p-values are indicated by insets in graphs). Light gray and dark gray backgrounds represent subjective day and subjective night, respectively, based on the phase analysis from **Figure 1D**. (C-E) Cultured astrocytes were transfected with the indicated siRNA (20nM) and processed for real-time qRT-PCR (C) and Western blot (D, E) analyses at 48hrs post transfection. (C) Values are mean ± SEM (n = 4; **p* < 0.05, ***p* < 0.005, ****p* < 0.0005, and *****p* < 0.00005; *t*-test). (D) Representative Western blot images of four independent experiments are shown. GAPDH served as loading control. (E) Densitometric quantification of HERP levels, normalized to GAPDH levels. Values are mean ± SEM (n = 4; ****p* < 0.0005; Mann-Whiteny *U* test). (F-I) Astrocyte cultures from rom WT (F, G) and *Bmal1*$^{-/-}$ (H, I) mice were synchronized and harvested at the indicated time for Western blot analysis. Total ERK (tERK) served as a loading control. HERP/tERK values at different times were normalized to those at 12hr post sync (set to 1). Meta2d *p* values are indicated by insets in graphs. Light gray and dark gray backgrounds represent subjective day and subjective night, respectively. (F) Representative Western blot images from five independent experiments are shown. (H) Representative Western blot images from two independent experiments are shown

daily cycles (**Figure 2F**) indicating strong circadian rhythms in cultured astrocytes. Importantly, HERP protein levels oscillated peaking at 18hr and 42hr and reaching a minimum at 12hr, 30hr, and 54hr, mirroring its mRNA pattern (**Figure 2F** and **2G**).

Herp also exhibited rhythmic expression in astrocyte cultures synchronized by either dexamethasone (Balsalobre et al., 2000) or forskolin (Yagita & Okamura, 2000) treatments which are other commonly used for circadian clock resetting (**Figure 2-figure supplement 1**). Finally, to investigate whether the rhythmic expression of *Herp* is regulated by a circadian clock, we examined *Herp* mRNA and protein expression patterns in primary astrocyte cultured from *Bmal1*$^{-/-}$ mice. The rhythmic expression patterns of *Per2*, *Rev- Erbα*, and *Herp* were abolished in *Bmal1*$^{-/-}$ astrocyte cultures with their expression maintained at trough levels (**Figure 2A**). HERP protein levels remained constant throughout the daily cycles (**Figure 2H** and **2I**). Collectively, these observations indicate that the expression of *Herp* exhibits a robust circadian rhythm that is controlled by BMAL1 in cultured mouse astrocytes. These results suggest that HERP-regulated cellular processes vary in a time-of-day specific manner.

Herp knockdown alters ATP-induced ER Ca^{2+} release

Herp was first identified as a gene with altered expression in response to homocysteine treatment in human umbilical vein endothelial cells (HUVECs) (Kokame et al., 1996). It is strongly induced not only by homocysteine but also by ER stress-causing agents such as tunicamycin or thapsigargin. HERP, characterized by an N-terminal ubiquitin-like domain and present in the ER membrane facing cytoplasmic side, is involved in the unfolded protein response (UPR) (Kokame et al., 2000) and is part of the ER- associated degradation (ERAD) complex, participating in the ubiquitination and relocation of ERAD substrates (Leitman et al., 2014). Notably, HERP modulates the ER Ca^{2+} response through IP_3R degradation (Paredes et al., 2016; Torrealba et al., 2017).

Thus, we sought to investigate whether HERP-controlled processes are subject to circadian regulation by examining the HERP-regulated ER Ca^{2+} response in the astrocytes. We employed the organelle-specific fluorescent Ca^{2+} indicators: G-CEPIA1er for the ER (Suzuki et al., 2014), R-GECO1 for the cytosol (Wu et al., 2013), and mito-R-GECO1 for mitochondria (Zhao et al., 2011). We first confirmed that these Ca^{2+} indicators colocalized with organelle-specific markers (**Figure 3-figure supplement 1**). ATP serves not only as a fundamental energy source but also as an active intercellular messenger. In astrocytes, ATP application induces an increase in intracellular Ca^{2+} (Neary et al., 1988) by binding to the G_q/G_{11} coupled P2Y receptor, activating PLC-β and inducing the hydrolysis of PIP_2 to diacylglycerol (DAG) and IP_3, which mobilizes Ca^{2+} through IP_3Rs on the ER membrane (Baryshnikov et al., 2003; James & Butt, 2001).

We treated control and *Herp*-KD astrocytes with 100μM ATP and monitored subcellular Ca^{2+} changes. ATP treatment rapidly decreased ER Ca^{2+} in control astrocytes and this response was more pronounced in *Herp*-KD astrocytes (**Figure 3A**-**3C**). As the main Ca^{2+} store in the cell, ER releases Ca^{2+} which is then rapidly transmitted to other organelles such as mitochondria and cytosol (Carreras-Sureda et al., 2018; Giorgi et al., 2018). Although ATP treatment did not significantly alter cytosolic Ca^{2+} signal in control astrocytes, it greatly increased cytosolic Ca^{2+} signals in *Herp*-KD astrocytes (**Figure 3D**-**3F**). Consistently, mitochondrial Ca^{2+} significantly increased in *Herp*-KD astrocytes compared with control (**Figure 3G**-**3I**).

Next, we examined the mechanism by which HERP controls ER Ca^{2+}.There are three subtypes of IP_3Rs encoded by the genes *Itpr1*, *Itpr2*, and *Itpr3*. Transcriptome analysis of our cultured astrocytes indicated *Itpr1* as the most prevalent, followed by *Itpr2*, while *Itpr3* expression was minimal (**Figure 3-figure supplement 2**). Notably, expression of these *Itpr* subtypes was not rhythmic. We then assessed the ITPR1 and ITPR2 protein levels in control and *Herp*-KD astrocytes and found that the levels of both ITPR1 and ITPR2 were slightly but statistically significantly

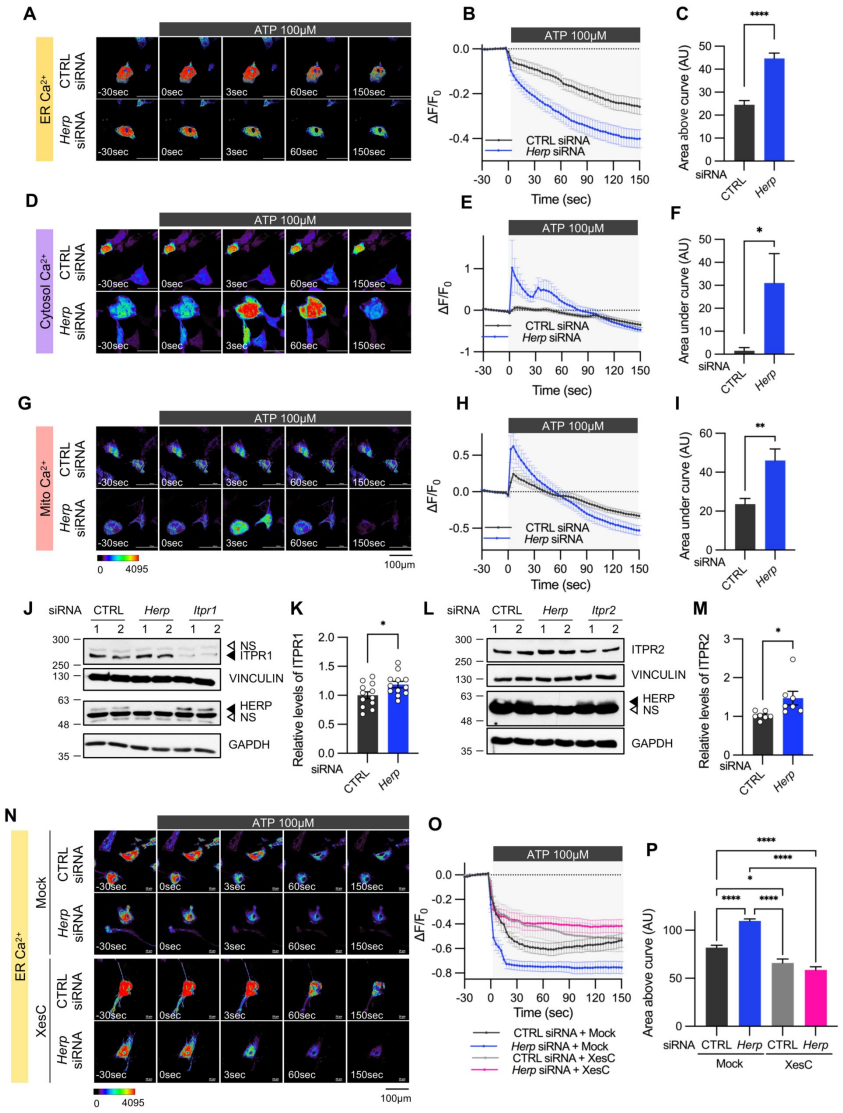

Figure 3.

Herp knockdown altered ATP-induced ER Ca^{2+} response.

(A-I) Cultured astrocytes were co-transfected with 20 μM non-targeting (CTRL) siRNA or *Herp* siRNA together with G-CEPIA1er (A-C), R-GECO1 (D-F) or mito-R-GECO1 (G-I). At 48hrs post transfection, cultured astrocytes were treated with 100 μM ATP and Ca^{2+} imaging analysis was performed. Images were acquired every 3 seconds. (A, D, G) Representative time-lapse images of each Ca^{2+} indicator. (B, E, H) $\Delta F/F_0$ values over time following ATP application. (C, F, I) Area above or area under the curve values, calculated from panels B, E, and H. (A-C) CTRL siRNA, n = 19; *Herp* siRNA, n = 22. (D-F) CTRL siRNA, n = 20; *Herp* siRNA, n = 25. (G-I) CTRL siRNA, n = 16; *Herp* siRNA, n = 16. (J-M) Cultured astrocytes were transfected with the indicated siRNA (20nM) and processed for Western blot analysis 48hrs post transfection. Vinculin and GAPDH served as loading control for ITPRs and HERP, respectively. (J) Representative Western blot images from twelve independent experiments are shown. NS, non-specific band (K) Densitometric quantification of Western blot data showing relative levels of ITPR1 in *Herp* siRNA-transfected astrocytes compared to CTRL siRNA transfected astrocytes. (L) Representative Western blot images from five independent experiments. (M) Densitometric quantification of Western blot data showing relative levels of ITPR2 in *Herp* siRNA-transfected astrocytes compared to Control astrocytes. Values are mean ± SEM (*$p < 0.05$, **$p < 0.005$, ***$p < 0.0005$, ****$p < 0.00005$; *t*-test). (N-P) Cultured astrocytes were treated with 10μM Xestospongin C (XesC), an IP3R inhibitor, for 30 minutes before live imaging. Cells were then treated with 100μM ATP, and images were captured every 3 seconds. (N) Representative time-lapse images of ER Ca^{2+} indicator. (O) $\Delta F/F_0$ values over time following ATP application. (P) Area above the curve values were calculated from panel B. CTRL siRNA + Mock, n = 9; *Herp* siRNA + Mock, n = 9 ; CTRL siRNA + XesC, n = 8; *Herp* siRNA+ XesC, n = 14. Values are means ± SEM (*$p < 0.05$, **$p < 0.005$, ***$p < 0.0005$, ****$p < 0.00005$; one-way ANOVA).

increased in *Herp*-KD astrocytes compared to controls (**Figure 3J**-**3M**). These results, consistent with previous reports (Paredes et al., 2016; Torrealba et al., 2017) indicated that HERP negatively regulates ITPRs in astrocyte.

To confirm that the HERP-ITPR axis underlies ER Ca^{2+} response, we analyzed the ER Ca^{2+} response following treatment with Xestospongin C (XesC), an IP3R inhibitor. XesC treatment reduced the ATP- induced ER Ca^{2+} release and abolished the enhanced effect observed in *Herp*-KD compared to control (**Figure 3N**-**3P**). Collectively, these results clearly indicate that HERP controls ER Ca^{2+} release by negatively regulating IP3Rs.

ATP-induced ER Ca^{2+} release varies according to time post synchronization

Given that HERP levels exhibited circadian variation and HERP regulated ER Ca^{2+} release, we investigated whether ATP-induced ER Ca^{2+} responses differ depending on circadian phase. After SS, we measured ER Ca^{2+} following ATP treatment at peak (42hr post sync) and trough (30hr post sync) phases of HERP (**Figure 4A**). With lower HERP levels potentially resulting in higher IP_3R levels at 30hr, we anticipated greater ER Ca^{2+} release at 30hr than at 42hr. Consistent with this, ER Ca^{2+} decreased more at 30hr than at 42hr upon ATP treatment (**Figure 4B**-**4D**). Also, in keeping with previous result (**Figure 3A**-**3I**), cytosolic Ca^{2+} increased more at 30hr than at 42hr following ATP treatment (**Figure 4E**-**4G**). Although mitochondrial Ca^{2+} responses exhibited a similar trend, the differences were not statistically significant (**Figure 4H**-**4J**).

To confirm that HERP underlies this circadian phase-dependent ER Ca^{2+} release, we compared ER Ca^{2+} release in control and *Herp*-KD astrocytes at 30hr and 42hr post sync. Control astrocytes exhibited time-dependent variation in ER Ca^{2+} release, which was abolished in *Herp*-KD astrocytes (**Figure 4K**-**4L**), indicating the involvement of HERP in this regulation.

We then assessed whether ITPR1 and ITPR2 levels varied with time. BMAL1 phosphorylation served as a proxy for circadian phase (**Figure 4N**). ITPR2 levels showed time-dependent changes opposite to those of HERP, whereas ITPR1 levels remained constant (**Figure 4N** and **4O**). Since *Itpr2* mRNA levels did not exhibit a rhythmic pattern (**Figure 3-figure supplement 1**), the circadian phase-dependent differences in ITPR2 levels are likely driven by HERP-mediated ITPR2 degradation. Consequently, circadian rhythmic ER Ca^{2+} release is primarily driven by oscillations in ITPR2.

To verify if ER Ca^{2+} release is regulated by the circadian clock, we analyzed the ER Ca^{2+} response in *Bmal1*$^{-/-}$mouse astrocyte cultures. In WT astrocyte cultures, there was a clear circadian phase-dependent difference in ER Ca^{2+} release. However, this difference was abolished in *Bmal1*$^{-/-}$ astrocyte cultures (**Figure 5A-C**). The absence of rhythmic ER Ca^{2+} release in *Bmal1*$^{-/-}$ astrocytes correlated with constant levels of HERP (**Figure 5D-E**). Additionally, ER Ca^{2+} release was significantly faster in *Bmal1*$^{-/-}$ astrocytes compared to WT astrocytes (**Figure 5A-C**) attributed to lower levels of HERP in *Bmal1*$^{-/-}$ astrocytes (**Figure 5D-E**). Collectively, these results indicate that ER Ca^{2+} release is regulated by HERP, which is under circadian clock control.

ATP-induced S368-phosphorylation of CX43 and gap junctional communication shows circadian variation

Syncytial coupling through gap junctions is a prominent feature of astrocytes, critical for their homeostatic functions, including the diffusion and equilibration of ions, metabolites, and signaling molecules (Langer et al., 2012; Verkhratsky & Nedergaard, 2018). This coupling allows the astrocytic syncytium to propagate Ca^{2+} waves, affecting nearby and remote cells through release of “gliotransmitters” and modulating synaptic functions in a far-reaching network (Pacholko et al.,

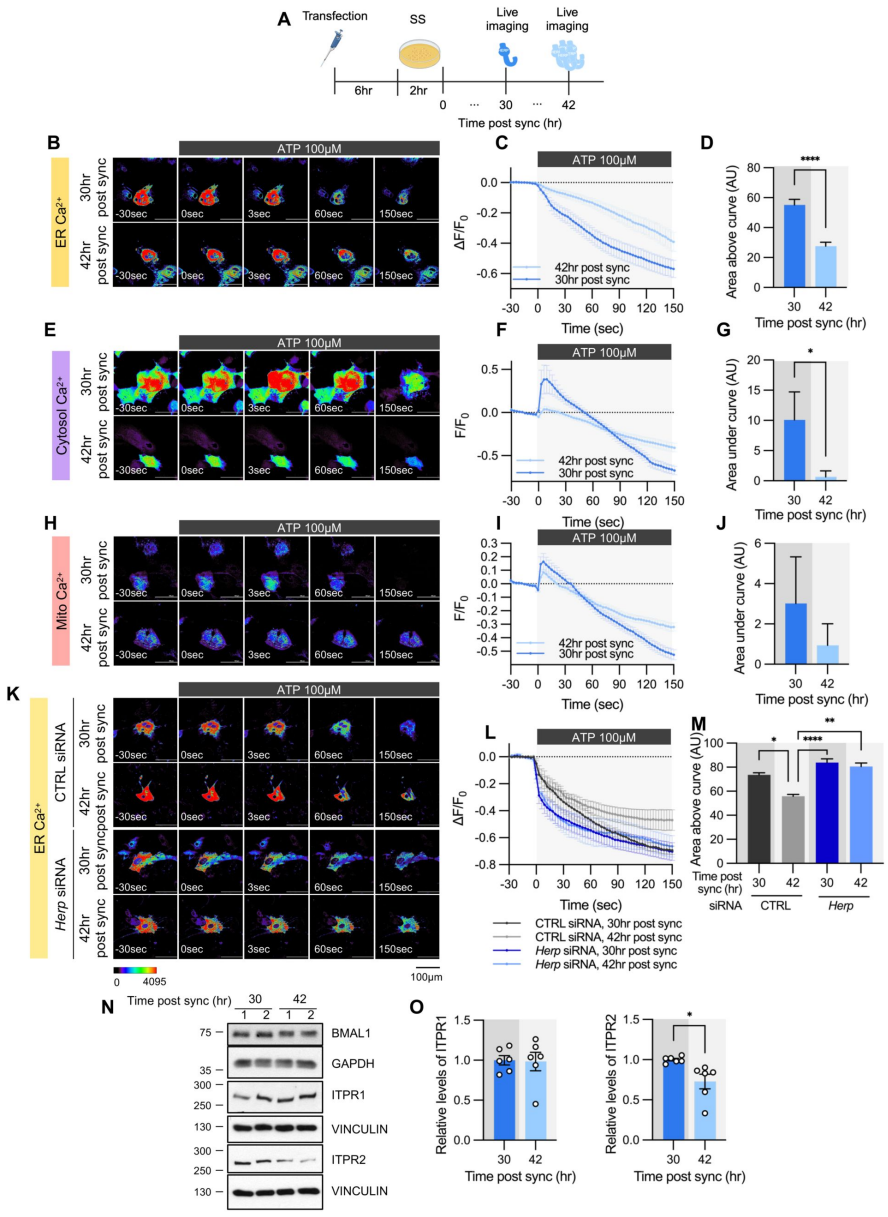

Figure 4.

ATP-induced ER Ca^{2+} release varies according to time post sync.

(A) Schematic diagram of the experimental scheme from transfection to live-cell Ca^{2+} imaging at different times. (B-M) Cultured astrocytes were transfected with G-CEPIA1er (B-D, K-M), R-GECO1 (E-G), or mito-R-GECO1 (H-J) compartment-specific Ca^{2+} indicators (denoted at left) and then their circadian rhythm was synchronized by SS. (K-M) The indicated siRNA was co-transfected with the ER Ca^{2+} indicator. After transfection, cells were allowed 48hrs for the siRNA to take effect and stabilize before synchronization by serum shock. At the indicated times, astrocytes were treated with 100 μM ATP and Ca^{2+} imaging was performed. (B, E, H, K) Representative time-lapse images of each Ca^{2+} indicator. (C, F, I, L) $\Delta F/F_0$ values over time following ATP application. (D, G, J, M) Area above or area under the curve values, calculated from panels C, F, I, and L. (B-D) 30hr post sync, n = 24; 42hr post sync, n = 19. (E-G) 30hr post sync, n = 33; 42hr post sync, n = 38. (H-J) 30hr post sync, n = 50; 42hr post sync, n = 54. (K-M) CTRL siRNA, 30hr post sync, n = 5; CTRL siRNA, 42hr post sync, n = 4; *Herp* siRNA, 30hr post sync, n = 11; *Herp* siRNA, 42hr post sync, n = 5. Values in graphs are mean ± SEM (*p < 0.05, ****p < 0.00005; (D, G, J) t-test, (M) one-way ANOVA. (N-O) Cells were harvested at the indicated times and processed for Western blot analysis. Vinculin and GAPDH served as loading controls for ITPR and BMAL1, respectively. (N) Representative Western blot images from six independent experiments. (O) Densitometric quantification of Western blot data showing relative levels of ITPR1 and ITPR2 at different times. Values in graphs are mean ± SEMs (*p < 0.05, ****p < 0.00005; t-test).

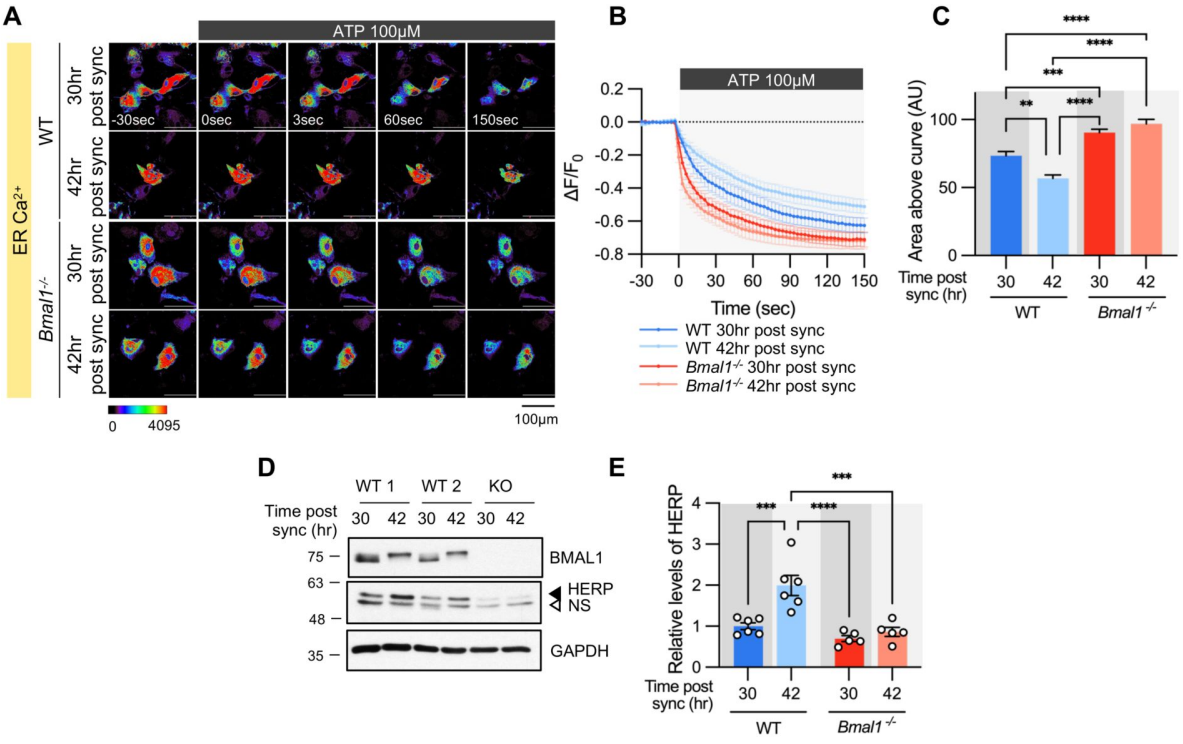

Figure 5.

Time-dependent ER Ca^{2+} release is abolished in cultured astrocytes from *Bmal1*$^{-/-}$mice.

Cultured astrocytes *Bmal1*$^{-/-}$ mice and WT littermates were transfected with G-CEPIA1er and then their circadian rhythm was synchronized by SS. At the indicated Time, astrocytes were treated with 100 μM ATP and Ca^{2+} imaging was performed. (A) Representative time-lapse images of ER Ca^{2+} indicator. (B) $\Delta F/F_0$ values over time following ATP application. (C) Area above the curve values, calculated from panel B. (A-C) WT 30hr post sync, n = 17; WT 42hr post sync, n = 15; KO 30hr post sync, n = 19; KO 42hr post sync, n = 21. Values are mean ± SEM (*p < 0.05, **p < 0.005, ***p < 0.0005, ****p < 0.00005; one-way ANOVA). (D, E) Cultured astrocytes from *Bmal1*$^{-/-}$mice and WT littermates were synchronized by SS. Cells were harvested at the indicated times and processed for Western blot analysis. (D) Representative Western blot images from six independent experiments. GAPDH served as a loading control. (E) Values are mean ± SEM (*p < 0.05, **p < 0.005, ***p < 0.0005, ****p < 0.00005; two-way ANOVA).

2020). Connexin (Cx) family proteins constitute gap junction channels (GJCs) (Giaume et al., 2021), with Cx43 (also known as Gja1) and Cx30 (also known as Gjb6) being the main connexins in astrocytes (Kunzelmann et al., 1999; Nagy et al., 1999). In our cultured astrocytes, Cx43 was the most abundantly expressed connexin (**Figure 6-figure supplement 1**). Phosphorylation of CX43 at Ser368 by protein kinase C (PKC), activated in response to intracellular Ca^{2+}, is known to decrease gap junction conductance (Enkvist & McCarthy, 1992; Nimlamool et al., 2015; Solan & Lampe, 2014). Accordingly, we hypothesized that the circadian variations in ATP-driven ER Ca^{2+} responses might differentially impact CX43 phosphorylation according to times of day.

First, we confirmed that ATP treatment induces rapid phosphorylation of CX43 at Ser368 (pCX43 (S368)) in cultured astrocytes (**Figure 6A** and **6B**). We then examined whether pCX43 (S368) varies with circadian phase. Notably, ATP-induced ER Ca^{2+} release was more pronounced at 30hr than at 42hr post sync (**Figure 3**), and pCX43 (S368) in response to ATP was also significantly higher at 30hr compared to 42hr post sync (**Figure 6C** and **6D**).

We also examined circadian variations of pCX43 (S368) *in vivo*. Mice were entrained to a 12:12 hour light/dark (LD) cycle for two weeks and then kept in constant darkness (DD). This ensured that variations in CX43 phosphorylation were due to the internal circadian clock and not external light stimuli. Prefrontal cortex tissues were dissected at circadian time (CT) 58 and CT70 on the third day of DD. pCX43 (S368) levels were higher at CT70 (subjective night) than at CT58 (subjective day), consistent with our *in vitro* results (**Figure 6E** and **6F**).

To confirm that HERP underlies the rhythmic phosphorylation of CX43 at Ser368, we compared pCX43 (S368) in control and *Herp*-KD astrocytes at 30hr and 42hr post sync. In control astrocytes pCX43 (S368) was higher at 30hr compared to 42hr, consistent with previous results. However, in *Herp*-KD astrocytes, the circadian phase-dependent differences in pCX43 (S368) were abolished despite the normal circadian rhythm indicated by BMAL1 phosphorylation, (**Figure 6G** and **6H**). This suggests that rhythms of HERP levels are required for the rhythmic phosphorylation of CX43 (S368).

Finally, we assessed if rhythmic phosphorylation of CX43 contributes to circadian phase-dependent variation in gap junctional communication in cultured astrocytes by using fluorescence recovery after photobleaching (FRAP) method. The absence of FRAP signal in carbenoxolone (CBX)-treated astrocytes confirmed the involvement of gap junctions in intercellular communication of cultured astrocytes (**Figure 7A**-**7C**). We observed a faster and more pronounced recovery of fluorescence in photobleached astrocytes at 42hr compared to 30hr post sync (**Figure 7D**-**7F**). Importantly, this variation was absent in astrocytes cultured from *Bmal1*$^{-/-}$ mice, indicating that circadian clock regulates gap junctional communication (**Figure 7G**.-**7I**).

In summary, we propose a model illustrating how the circadian clock influences astrocyte function through the regulation of ER Ca^{2+} response. Based on phase comparisons of clock genes between our data and CircaDB (**Figure 1D**), we defined subjective day and night, with 8hr post sync corresponding to the beginning of the day. In astrocytes, BMAL1/CLOCK-controlled oscillation of HERP regulates day and night variations in ITPR2 levels. These oscillations contribute to changes in ER Ca^{2+} responses, which in turn result in the distinct day and night differences in pCx43 (S368) and the gap junction conductance (**Figure 7J**).

Discussion

It is widely acknowledged that the circadian clock orchestrates cellular functions in a highly cell type-specific manner by governing transcription (Mure et al., 2018; Zhang et al., 2014). Although the importance of the circadian clock in astrocytes has been well-documented (Barca-

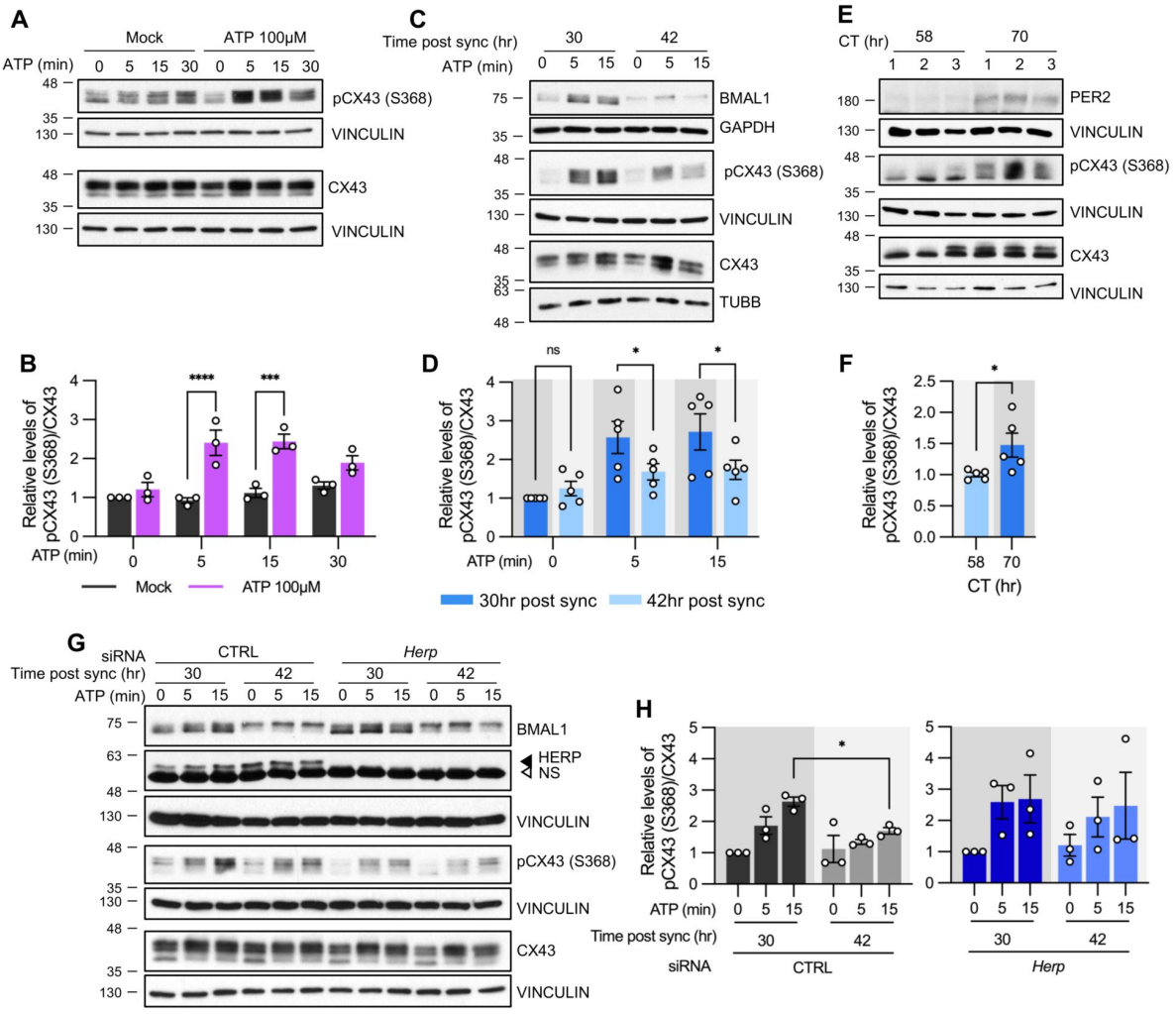

Figure 6.

ATP-induced pCX43 (S368) levels varies according to time post sync.

(A-D, G, H) Cultured astrocytes with (C, D) or without (A, B) synchronization, were treated with 100 μM ATP either at 30hr post sync or 42hr post sync and processed for Western blot analysis at the indicated times. Vinculin, GAPDH, and/or β-tubulin (TUBB) served as loading controls. The intensity of pCX43 (S368) and Cx43 for each sample was normalized to that of Vinculin. (A) Representative Western blot images from more three independent experiments. Vinculin served as a loading control. (B) Densitometric quantification of Western blot data, showing relative pCX43 (S368)/CX43 levels. Values are normalized to those for mock-treated samples at time zero (set to 1). (C) Representative Western blot images from three independent experiments. Vinculin, GAPDH, and β-tubulin (TUBB) served as loading controls. (D) Densitometric quantification of Western blot data, showing relative pCX43 (S368)/CX43 levels. Values are normalized to those for mock-treated samples at ATP zero for 30hr post sync (set to 1). (E, F) Changes in CX43 phosphorylation in vivo. Mice were entrained to a 12-hour light/dark cycle followed by constant dark conditions. At the indicated times, the prefrontal cortex area was dissected and processed for Western blot analysis. (E) Representative Western blot images from three independent experiments. (F) Densitometric quantification of Western blot data showing relative levels of pCX43 (S368). (G, H) 48hrs post siRNA transfection, cells were synchronized by serum shock. At the indicated times post sync, 100 μM ATP was treated and processed for Western blot analysis (G) Representative Western blot images from three independent experiments. Vinculin served as a loading control. (H) Densitometric quantification of Western blot data, showing relative pCX43 (S368)/CX43 levels. Values are normalized to those for 30hr post sync at ATP zero (min) (set to 1). Values are mean ± SEM (*$p < 0.05$, **$p < 0.005$, ***$p < 0.0005$, ****$p < 0.00005$; (B, D, H) two-way ANOVA, (F) *t*-test).

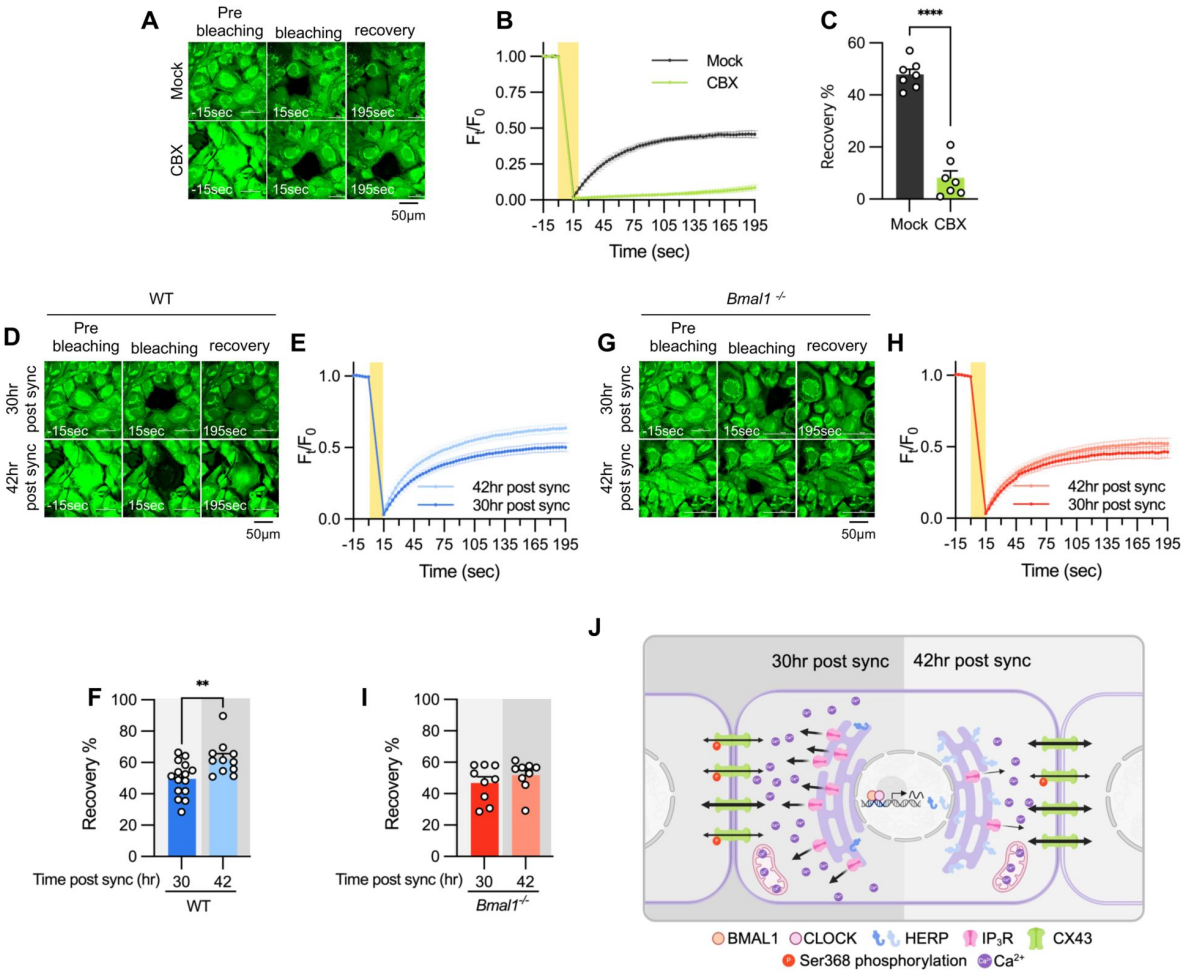

Figure 7.

Gap junction conductance varies according to time post sync.

(A-C) 20μM carbenoxolone (CBX), a gap junction channel block, was applied to cultured astrocytes for 30 minutes before gap-FRAP analysis. (A) Representative time-lapse images of prebleaching, bleaching and recovery condition during gap-FRAP analysis. (B) F_t/F_0 values over time following photobleaching (yellow rectangle). (C) Recovery % values, calculated from panel B. Mock, n = 7; CBX, n = 7. Values in graphs are mean ± SEM (*p < 0.05, **p < 0.005, ***p < 0.0005, and ****p < 0.00005; Mann-Whitney U test). (D-I) Cultured astrocytes from WT (D-F) and *Bmal1*$^{-/-}$ (G-I) mice were synchronized by SS. At the indicated time, gap-FRAP was performed. (D, G) Representative time-lapse images of prebleaching, bleaching and recovery condition during gap-FRAP analysis at 30hr post sync and 42hr post sync. (E, H) F_t/F_0 values over time following photobleaching (yellow rectangle). (F and I) Recovery % values, calculated from panel H and L, respectively. (D-F) 30hr post sync, n = 15; 42hr post sync, n = 11. (G-I) 30hr post sync, n = 9; 42hr post sync, n = 9. Values in graphs are mean ± SEM (*p < 0.05, **p < 0.005, ***p < 0.0005, and ****p < 0.00005; F : t-test, I : Mann-Whiteny U test). (J) Schematic diagram illustrating the regulation of ER Ca^{2+} response by the circadian clock through rhythmic oscillation of HERP. Refer to the text for the detailed explanation.

Mayo et al., 2020; Barca-Mayo et al., 2017; Griffin et al., 2019; Lananna et al., 2018; Prolo et al., 2005; Tso et al., 2017), studies specifically exploring astrocyte-specific circadian transcriptomes have been limited. Our study conducted such an analysis on primary cultured cortical astrocytes, discovering that rhythmic expression of *Herp* underlies day/night variation in ER Ca^{2+} response by regulating IP_3R levels. We also found that Ca^{2+}-activated CX43 phosphorylation varied according to the daily rhythmic ER Ca^{2+} response. Given that astrocytes function in a network in which Ca^{2+} propagates through GJCs, we propose that the time-dependent control of ER Ca^{2+} responses could influence the role of astrocytes in modulating synaptic activity throughout the day (see below).

Circadian oscillations of *Herp* expression have been previously documented in various mouse tissues including the lung, heart, liver, kidney, aorta, skeletal muscle, adrenal gland, pancreatic islet and SCN (Panda et al., 2002; Rakshit et al., 2016; Zhang et al., 2014). In this study, we identified that *Herp* is also rhythmically expressed in cultured astrocytes. *Herp* exhibited rhythmic expression in phase with *Per2* and showed flattened expression at its nadir level in *Bmal1*$^{-/-}$ astrocyte cultures, suggesting direct regulation CLOCK/BMAL1 heterodimers (**Figure 2A**). ChIP-Atlas analysis (*https://chip-atlas.org*) (Oki et al., 2018; Zou et al., 2022) has shown CLOCK binding to the genomic region of *Herp* (Annayev et al., 2014; Hong et al., 2018). Although no canonical E-Box is present in the upstream 6kb region of the *Herp* gene, several non-canonical E-Boxes, important for circadian expression (Yoo et al., 2005; Zhang et al., 2011), were identified (**Table S2**). Among these, the non-canonical E-Box sequence "CACGTT," located near transcription start site (chr8:94386194-94386543), is highly conserved across diverse mammalian species. Therefore, we propose that these non-canonical E boxes might drive the CLOCK/BMAL1 dependent expression of *Herp*. A recent study employing a circadian single-cell RNA seq analysis of SCN reported that *Herp* displays a circadian rhythm exclusively in astrocytes and oligodendrocytes (Wen et al., 2020). Given that astrocytic Ca^{2+} levels in the SCN show a circadian rhythm, peaking during the subjective night and are crucial for circadian timing (Brancaccio et al., 2019; Patton et al., 2022), HERP's circadian rhythmic expression in SCN astrocytes (Wen et al., 2020) may be integral to the mechanisms of circadian timing.

We demonstrated that HERP regulated ER Ca^{2+} responses by degrading IP_3Rs in astrocytes (**Figure 3J-3M**). (Paredes et al., 2016; Torrealba et al., 2017). When *Herp* was downregulated, both ITPR1 and ITPR2 levels increased, suggesting HERP's role in degrading both ITPR1 and ITPR2. However, only the levels of ITPR2 exhibited circadian phase-dependent variation (**Figure 3J-3M**, **Figure 4K-4L**). The min/max ratio of HERP expression throughout the day was 0.38 under normal conditions but 0.072 in *Herp*-KD conditions. Based on this, we reasoned that the amplitude of HERP oscillations impacted the levels of ITPR2 under normal circumstances, while having a much lesser effect on the levels of ITPR1. Thus, the circadian control of ER Ca^{2+} release in response to stimulation in cultured astrocytes is primarily attributable to ITPR2.

ER and cytosolic Ca^{2+} responses following ATP treatment exhibited distinct circadian variation, but mitochondrial Ca^{2+} responses did not show significant variations (**Figure 4**). We think of several possibilities to account for the absence of significant circadian variations in mitochondrial Ca^{2+} relative to cytoplasmic Ca^{2+} change. Upon ATP stimulation, direct Ca^{2+} transfer occurs through IP_3R in the cytosol. For mitochondrial uptake, Ca^{2+} first transits to the intermembrane space via IP_3Rs and the voltage-dependent anion channel (VDAC) complex before entering the matrix through mitochondrial calcium uniporter (MCU) (Giorgi et al., 2018). The Mito-R-GECO1 reporter is confined within the mitochondrial matrix and thus limiting assessment of Ca^{2+} levels in the intermembrane space (Wu et al., 2013). Substantial changes in Ca^{2+} levels might occur in the intermembrane space, but the influx into the matrix via MCUs could remain constant across different time, resulting in apparent lack of significant change. Secondly, the amount of VDAC or the VDAC:IP_3R complex on the mitochondrial membrane might vary inversely with HERP levels, potentially maintaining a consistent flow of Ca^{2+} into the mitochondria irrespective of the time. Additionally, the presence of several Ca^{2+} extrusion mechanisms in mitochondria (Giorgi et al.,

2018) points to a more complex regulation of Ca^{2+} compared with that in the cytosol. Although the precise mechanism remains to be elucidated, our data indicate that the circadian variation in Ca^{2+} release from the ER, particularly in response to stimuli, predominantly impacts cytoplasmic signaling rather than mitochondrial signaling.

During the subjective night phase (active period for mice), ATP- stimulated ER Ca^{2+} release was pronounced than during the subjective day phase (rest period for mice) (**Figure 4**). This finding aligns with studies showing heightened stimulus-evoked Ca^{2+} activity in astrocytes during wakefulness, which diminishes during sleep (Bojarskaite et al., 2020; Ingiosi et al., 2020). In flies, Ca^{2+} activity in astrocytes is correlated with the duration of wakefulness, suggesting that astrocytic Ca^{2+} is a key factor in the homeostatic regulation of sleep (Blum et al., 2021). Our findings provide a mechanistic explanation for differential Ca^{2+} levels observed between wake and sleep states, with circadian regulation of ITPR2 by HERP being a key factor in this process.

ATP-stimulated Cx43 (S368) phosphorylation is higher at 30hr (subjective night phase) than at 42hr post sync (subjective day phase) (**Figure 6C** and **6D**.), a finding further supported by in *vivo* experiments (**Figure 6E** and **6F**). What are the implications of this day/night variation in CX43 (S368) phosphorylation? We reasoned that the circadian variation in CX43 phosphorylation could significantly impact astrocyte functionality within the syncytium. Indeed, our cultured astrocytes exhibited circadian phase-dependent variation in gap junctional communication (Figure7D-7F). Astrocytes influence synaptic activity through the release of gliotransmitters such as glutamate, GABA, D-serine, and ATP, triggered by increases in intracellular Ca^{2+} in response to the activity of adjacent neurons and astrocytes (Verkhratsky & Nedergaard, 2018). Importantly, this increase in Ca^{2+} spreads to adjacent astrocytes through GJCs (Fujii et al., 2017), influencing a large area of the neuronal network. Considering that Cx43 Ser368 phosphorylation occurs to uncouple specific pathways in the astrocytic syncytium to focus local responses (Enkvist & McCarthy, 1992), our findings suggest that astrocytes better equipped for localized responses when presented with a stimulus during the active phase in mice. Conversely, during the rest period, characterized by more synchronous neuronal activity across broad brain areas (Vyazovskiy et al., 2009) higher GJC conductance might allow astrocytes to exert control over a larger area. In support of this idea, recent study showed that synchronized astrocytic Ca^{2+} activity advances the slow wave activity (SWA) of the brain, a key feature of non-REM sleep (Szabó et al., 2017). Blocking GJC was found to reduce SWA, further supporting this interpretation. However, conflicting findings have also been reported. For instance, Ingiosi et al. (Ingiosi et al., 2020) found that astrocytic synchrony was higher during wakefulness than sleep in the mouse frontal cortex. Whether these differing results in astrocyte synchrony during resting and active periods are attributable to differences in experimental context (e.g., brain regions, sleep-inducing condition) remains unclear. Indeed, astrocyte Ca^{2+} dynamics during wakefulness/sleep vary according to brain regions (Tsunematsu et al., 2021). While the extent of astrocyte synchrony might differ depending on brain region and/or stimulus, our results suggest that the baseline state of astrocyte synchrony, which is affected by GJC conductance, varies with the day/night cycle.

In conclusion, our findings enhance the understanding of the circadian regulation of astrocytic functions, particularly through the rhythmic expression of HERP and its impact on ER Ca^{2+} signaling and CX43 phosphorylation. This study underscores the intricate interplay between the circadian clock and astrocyte physiology, highlighting the pivotal role of HERP in modulating key astrocytic processes such as sleep, gap junction communication and synaptic modulation. The day/night variations in ER Ca^{2+} response and CX43 phosphorylation, and their implications for astrocytic network dynamics and neuronal interactions, open new avenues for exploring the broader implications of astrocytic circadian rhythms in brain function and health.

Materials and Methods

Animals

All procedures for the care and use of laboratory animals were approved by the Institutional Animal Care and Use Committee (IACUC) of Ajou University School of medicine. *Bmal1*$^{-/+}$ mice (B6.129-Bmal1^{tm1Bra}/J; Jackson Laboratory, #009100)(Bunger et al., 2000) were purchased from Jackson Laboratory(USA) and housed in a specific pathogen-free environment at the Animal Research Center of Ajou University Medical Center, with a standard 12-hour light/dark cycle and free access to food. Primary cultured astrocytes involving only WT mice used 1day-old C57BL/6 mice (Koatch Inc., Korea). In experiments employing primary cultured astrocytes from *Bmal1*$^{-/-}$ mice, wild type (WT) littermates were used as controls. For animal studies, 7-8 week-old adult C57BL/6 male mice were first entrained in a standard 12-hour light/dark cycle for 2 weeks and then maintained in a constant darkness (DD). On the third day of DD, mice were sacrificed at indicated time and its prefrontal cortex (PFC) was dissected.

Primary astrocyte culture

Primary astrocyte culture was prepared according to a previous report (Choi et al., 2018) with minor modifications. In brief, 1 day old pups were anesthetized by hypothermia and their cerebral cortices were dissected out and triturated in Modified Eagle's medium (MEM; Welgene, Korea, LM 007-11) containing 10% fetal bovine serum (FBS; Hyclone, USA, SV30207.02), penicillin/streptomycin (Gibco, USA, 15140-122), 10 μM HEPES (Gibco, USA, 15630080) and GlutaMAX (Gibco, USA, 35050-061) yielding a single-cell suspension. Cells were plated into 75 cm^2 T-flasks (1pup/flask) and incubated at 37°C in a humidified 5% CO_2 incubator for 2 weeks. Primary astrocytes were then incubated in a serum-free MEM for 7 days, after which astrocytes were detached from the T-flask with 0.25% trypsin and plated on culture dishes (1.0X10^6cells/60 mm dish) for experiments.

Circadian transcriptome analysis

The experimental scheme for synchronizing circadian clocks of cultured astrocyte is illustrated in **Figure 1A**. In brief, astrocytes were grown in dishes (1.0 X 10^6cells/60 mm dish) until reaching complete confluence and then incubated in serum-free MEM for 72hrs. Cells were then subjected to serum shock (SS), a well-established procedure for synchronizing the circadian clock of cultured cells (Balsalobre et al., 1998), by exchanging the medium for MEM containing 50% horse serum. 12hrs post SS, astrocytes were harvested at 4-h intervals for 2 days for RNA sequencing (RNA-seq). Total RNA was extracted and purified from harvested astrocytes using a RNeasy Plus Micro Kit (Qiagen, Germany, 74034). RNA quality and quantity assessments, RNA-Seq library construction, and next-generation sequencing analysis were performed by Macrogen Inc. (Korea). Total RNA integrity and library size were analyzed using an Agilent Technologies 2100 Bioanalyzer. Paired-end raw reads, generated using an Illumina HiSeq 2000 system, were aligned to the mm10 mouse genome using STAR aligner (v.2.5.2b)(Dobin et al., 2013). Gene expression was subsequently quantified by calculating transcripts per million (TPM) using Ensemble gene (release 82) annotations. The threshold for defining expressed transcripts was set using a Gaussian mixture model in the R package 'mixtools'. To detect circadian oscillating transcripts, we employed two circadian oscillation detection methods BioCycle (Agostinelli et al., 2016) and MetaCycle (Wu et al., 2016).

Quantitative reverse transcription polymerase chain reaction (qRT-PCR)

Total RNA was extracted from cells and purified using the RNeasy Plus Micro Kit (Qiagen, 74034). 1μg of total RNA was reverse transcribed using an oligo-dT primer and PrimeScript RTase (TaKaRa, Japan, 2680A). Quantitative real-time PCR was performed using a Rotor Gene Q (Qiagen) with TB Green Premix Ex Taq (Takara, RR420A) The specific primers used were provided in the **Table S3**. Noncycling mRNA encoding HPRT was used to normalize gene expression. The data were analyzed using Rotor Gene 6000 software, and the relative mRNA levels were quantified using the $2^{-\Delta\Delta Ct}$ method in which $\Delta\Delta Ct=[(Ct_{target} - Ct_{HPRT})$ of experimental group]-[$(Ct_{target} - Ct_{HPRT})$ of control group].

siRNA transfection and Immunoblotting

The following On-Target plus SMARTpool siRNAs were purchased from Dharmacon (USA): Non-targeting CTRL siRNA (D-001810-01-50), *Herp* siRNA (L-049714-01-0005), *Itpr1* siRNA (L-040933-00-0005), and *Itpr2* siRNA (L-041018-00-0005). Upon reaching >90% confluence, the medium was replaced with serum-free MEM, and cells were incubated for 72hrs. Cells were then transfected with siRNA using Lipofectamine RNAiMAX (ThermoFisher, USA, 13778150) per the manufacturer's instructions. Experiments were conducted 48hrs post-transfection.

For immunoblotting, astrocytes were lysed using modified-RIPA buffer (50 mM Tris-HCl pH 7.4, 1% NP-40, 0.5% sodium deoxycholate, 150 mM NaCl). Mouse prefrontal cortex was lysed using T-Per (ThermoFisher, 78510) with protease inhibitor cocktail (Sigma-Aldrich, P8340) and phosphatase inhibitor cocktails 2 and 3 (Sigma-Aldrich, P5726 and P0044). Proteins were separated by SDS-PAGE and transferred to polyvinylidene fluoride membranes. Membranes were blocked with 5% skim milk and incubated overnight at 4°C with primary antibodies: anti-BMAL1 (Abcam (UK), ab93806), 1:2000; anti-HERP (Abcam, ab150424), 1:1000; anti-ITPR1 (Abcam, ab264284), 1:1000; anti-ITPR2 (Alomone Labs, Israel, ACC-116), 1:1000; anti-CX43 (Sigma, C6219), 1:5000; anti-pCX43 (Ser368) (CST, USA, 3511), 1:1000; anti-GAPDH (Novus, USA, NB100-56875), 1:5000; anti-vinculin (Sigma-Aldrich, V4505), 1:5000; and anti-total ERK (CST, 9102), 1:5000. Membranes were washed with TBST, incubated with secondary antibodies, and visualized using enhanced chemiluminescence. Protein levels were quantified by densitometric analysis of band intensities using ImageJ software.

Ca^{2+} reporter plasmid transfection and imaging analysis

After cells reached >90% confluence, the medium was replaced with serum-free MEM. For Ca^{2+} measurements, cells were transfected with Ca^{2+} indicator plasmids pCMV-G-CEPIA1er (a gift from Masamitsu Iino, Addgene plasmid #58215) (Suzuki et al., 2014), CMV-mito-R-GECO1, or CMV-R-GECO1 (gifts from Robert Campbell, Addgene plasmid #46021, #32444) (Wu et al., 2013) 72hrs post-serum deprivation using Lipofectamine 2000, with or without siRNA treatment. For Xestospongin C (XesC) experiments, 10 μM XesC was applied 30 minutes before imaging. 48hrs post-transfection, the medium was replaced with Ca^{2+}- and Mg^{2+}-free HBSS (Gibco, 14175095). Fluorescence images were captured every 3 seconds using a Nikon A1R Confocal Microscope with a x60 1.4 NA Plan-Apochromat objective at 37°C and 5% CO2. These experiments were conducted at the Three-Dimensional Immune System Imaging Core Facility of Ajou University (Korea). Images were analyzed using NIS Elements C software. Fluorescence intensity at each time point (F_t) and ΔF values (F_t-F_0) were calculated. F_0 values were averaged from the fluorescence intensity of 10 frames prior to stimulation.

Ca^{2+} reporter plasmid co-localization analysis

After cells reached >90% confluence, the medium was replaced with serum-free MEM. 72hrs later, cells were transfected with either the ER Ca^{2+} reporter plasmid pCMV-G-CEPIA1er or the mitochondrial Ca^{2+} reporter CMV-mito-R-GECO1. For ER co-localization analysis, pCMV-G-CEPIA1er was co-transfected with DsRed2-ER-5 (a gift from Michael Davidson, Addgene plasmid #55836) (Day & Davidson, 2009). For mitochondrial co-localization, 200 nM Mitotracker was applied 30 minutes before imaging. Live imaging was performed using a Nikon A1R Confocal Microscope with a x60 1.4 NA Plan-Apochromat objective at 37°C and 5% CO2. These experiments were conducted at the Three-Dimensional Immune System Imaging Core Facility of Ajou University (Korea). Images were analyzed using NIS Elements C software.

Gap-FRAP (fluorescence recovery after photobleaching) analysis

Astrocyte communication was evaluated using a modified gap-FRAP assay (Santiquet et al., 2012). 30 minutes before imaging, cells were incubated with 0.5 μM Calcein-AM (Invitrogen, C1430) and 0.05% Pluronic-127 (Invitrogen, P6866) at 37°C. After incubation, cells were rinsed twice with serum-free MEM to remove excess dye. For carbenoxolone (CBX) experiments, 20 μM CBX was added for 30 minutes after calcein incubation. Immediately before imaging, the medium was replaced with Ca^{2+}- and Mg^{2+}-free HBSS (Gibco, 14175095). Live imaging was performed using a Nikon A1R Confocal Microscope with a 488 nm argon laser and a x60 1.4 NA Plan-Apochromat objective. Photobleaching was performed on a region of interest (ROI) cell, and fluorescence was measured at 37°C and 5% CO2. Fluorescence intensity was recorded pre-bleach (5 images), during a 15-second laser pulse (100% power, 5.3 lines/sec), and post-bleach (every 3 seconds for 3 minutes). Images were analyzed using NIS Elements C software. Fluorescence intensity at each time point (F_t) was normalized to the pre-bleach intensity (F_0), calculated as the average of 5 pre-bleach frames. The percentage of fluorescence recovery was calculated using: $(F_{FR}-F_A)/(F_0-F_A)x100$, where F_{FR} is the full recovery fluorescence intensity and F_A is the intensity immediately after photobleaching.

Quantification and statistical analysis

To conduct the statistical analyses, all samples were first tested for normality. For cases where normality testing was not possible, such as with the Area Under/Above Curve, *t*-tests were used for comparing two groups, and one-way ANOVA was used for comparing three or more groups, considering the sufficient sample size. When comparing two groups, a *t*-test was performed if the data followed a normal distribution; otherwise, the Mann-Whitney *U* test was used. For comparisons among three or more groups, one-way ANOVA was used if the data were normally distributed, and the Brown-Forsythe and Welch ANOVA tests were used if they were not. When comparing three or more groups across multiple time points, a two-way ANOVA was performed. A $p < 0.05$ was considered statistically significant for all tests.

Data and code availability

- Circadian RNA sequencing data have been deposited at GEO under accession number GEO: GSE254678.
- Any additional information required to reanalyze the data reported in this paper is available from the E.Y.K upon request.

Acknowledgements

We are very grateful to Eunhye Joe and all members of Eun Young Kim's laboratory for critical comments on the manuscript. This research was supported by National Research Foundation of Korea (NRF) grants funded by the Korean government (Ministry of Science and ICT; grant numbers, 2019M3C7A1031905, 2019R1A5A2026045).

Additional information

Author Contributions

J.E.R., H.W.R., J.L., and E.Y.K designed research. J.E.R., K. S., H.W.R., and J.L. performed research. All authors analyzed data. J.E.R. and E.Y.K. wrote the first draft of the manuscript and all authors contributed to revising the manuscript.

Declaration of interests

The authors declare no competing interests.

Supplemental information

	MetaCycle		BioCycle		
Gene	p value	Amplitude	p value	Amplitude	Average TPM[a]
Herp	2.14E-09	11.66	0.00000001	11.35	71.13
Slc4a11	3.22E-09	1.48	0.00000100	1.50	6.68
Sord	3.60E-08	3.60	0.00002116	4.22	42.26
Kcnh1	5.50E-06	0.52	0.00000729	0.40	0.96
Anxa7	6.04E-06	4.44	0.00001444	4.23	102.07
Cx3cl1	3.13E-05	8.76	0.00019881	8.00	80.19
Pik3r1	5.21E-05	2.75	0.00126025	3.17	35.69
Hfe	0.000105052	2.94	0.00001600	2.95	32.10
Nr4a3	0.000106683	2.17	0.00064009	1.94	19.54
Spp1	0.000111664	31.47	0.00978121	41.58	168.53
Nppc	0.000162403	1.71	0.00017424	2.02	11.79
Sumo1	0.000462997	11.16	0.01687401	10.88	128.46
Tns2	0.000494944	1.01	0.00220900	1.21	13.15
Steap3	0.00050386	3.35	0.00494209	2.73	24.42
Capn1	0.000693268	2.57	0.00368449	2.49	48.74
Syt1	0.000707495	0.40	0.00015129	0.29	2.42
Ank	0.000906762	12.09	0.00077284	11.49	220.39
Casq2	0.001722008	0.67	0.00036864	0.64	5.78
Kcnj10	0.003437489	41.65	0.00088804	35.76	485.66
Adora1	0.005727835	6.56	0.00000009	7.08	63.08
P2ry1	0.006372537	1.77	0.00013225	1.99	19.40
Pcgf2	0.020637656	1.69	0.00090601	1.40	31.54
Dgat2	0.032505924	1.49	0.00055225	1.61	15.48

[a]Of all Time-merged values

Table S1.

Calcium ion homeostasis

E-box type	start position	end position	Upstream position	sequence	position
CANNTG	94380510	94380515	-5928	CATCTG	chr8:94380510-94380515
CANNTG	94381181	94381186	-5257	CAAGTG	chr8:94381181-94381186
CANNTG	94381199	94381204	-5239	CAGCTG	chr8:94381199-94381204
CANNTG	94381442	94381447	-4996	CAATTG	chr8:94381442-94381447
CANNTG	94381536	94381541	-4902	CAAGTG	chr8:94381536-94381541
CANNTG	94381563	94381568	-4875	CAGATG	chr8:94381563-94381568
CANNTG	94381689	94381694	-4749	CAAATG	chr8:94381689-94381694
CANNTG	94381721	94381726	-4717	CATCTG	chr8:94381721-94381726
CANNTG	94382162	94382167	-4276	CAATTG	chr8:94382162-94382167
CANNTG	94382173	94382178	-4265	CACCTG	chr8:94382173-94382178
CANNTG	94382368	94382373	-4070	CAGGTG	chr8:94382368-94382373
NC-CAGCTT	94382386	94382391	-4052	CAGCTT	chr8:94382386-94382391
CANNTG	94382714	94382719	-3724	CACCTG	chr8:94382714-94382719
CANNTG	94382896	94382901	-3542	CAGCTG	chr8:94382896-94382901
CANNTG	94383317	94383322	-3121	CATATG	chr8:94383317-94383322
CANNTG	94383445	94383450	-2993	CAGATG	chr8:94383445-94383450
CANNTG	94384166	94384171	-2272	CAAGTG	chr8:94384166-94384171
CANNTG	94384284	94384289	-2154	CATTTG	chr8:94384284-94384289
NC-CACGTT	94384539	94384544	-1899	CACGTT	chr8:94384539-94384544
CANNTG	94384874	94384879	-1564	CAAATG	chr8:94384874-94384879
CANNTG	94384902	94384907	-1536	CACATG	chr8:94384902-94384907
CANNTG	94385063	94385068	-1375	CAGCTG	chr8:94385063-94385068
CANNTG	94385102	94385107	-1336	CAAATG	chr8:94385102-94385107
CANNTG	94385331	94385336	-1107	CAGGTG	chr8:94385331-94385336
CANNTG	94385353	94385358	-1085	CATGTG	chr8:94385353-94385358
NC-CAGCTT	94385511	94385516	-927	CAGCTT	chr8:94385511-94385516
CANNTG	94385809	94385814	-629	CAGATG	chr8:94385809-94385814
CANNTG	94385910	94385915	-528	CACTTG	chr8:94385910-94385915
NC-CACGTT	94386384	94386389	-54	CACGTT	chr8:94386384-94386389

Table S2.

***Herp* upstream 6kb region non-canonical E-Box**

Table S3

Table of primers used in quantitative RT-PCR

Primers	SOURCE
Bmal1 F: CAC CTA ATT CTC AGG GCA G	Marcrogen
Bmal1 R: CAC CTA ATT CTC AGG GCA G AGA CTC GGA GAC AAA GAG G	Marcrogen
Nr1d1(Rev-erb α) F: AAT GTT CTG CTG GCA TGT C	Marcrogen
Nr1d1(Rev-erb α) R: GAA GTC TTC CCA GAT CTC CT	Marcrogen
Hprt F: GATTAGCGATGATGAACCAGGT	Marcrogen
Hprt R: CCTCCCATCTCCTTCATGACA	Marcrogen
Herp F: GGT GGA GGA AGA TGA TGA GAT AAA	Marcrogen
Herp R: CTC AGC GAG GAG TAG AAG TAA AG	Marcrogen

Figure 1-figure supplement 1.

Identification of circadian rhythmic transcripts in mouse cultured astrocytes

(A) Histogram showing the distribution of mean expression levels of transcripts. Transcripts with low (red) and high (green) expression were identified using a Gaussian mixture model. Dashed vertical lines represent cut-off points for highly expressed transcripts: maroon line (99.5%, TPM 0.40), blue line (99.0%, TPM 0.57), and purple line (95.0%, TPM 1.59). (B) Time-averaged expression levels of marker genes for astrocytes, microglia, oligodendrocytes, neurons, and endothelial cells in astrocyte cultures. Values are mean TPM ± S.E.M (n = 2); *, not detected. (C) Expression profiles of *Plat*, *Il34*, *Adora1*, and *Mybph* in SS-synchronized cultured astrocytes from RNA-seq data. The q-values for BioCycle (red) and MetaCycle (blue) are shown in the bottom right corner. (D) Heatmap of 412 candidate genes from RNA-seq data, ordered by MetaCycle phase. Expression levels were normalized using Min-Max normalization.

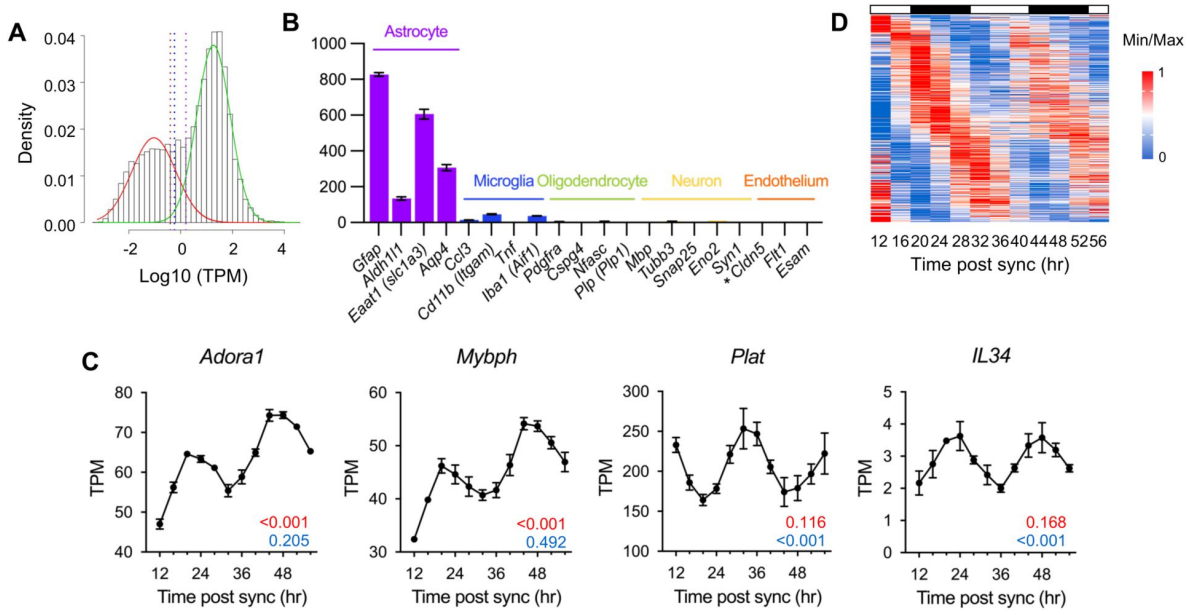

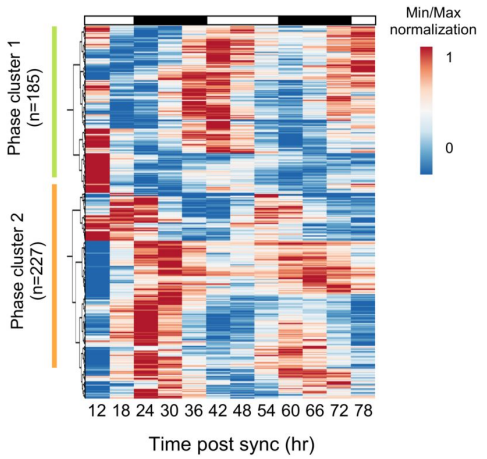

Figure 1-figure supplement 2.

Cluster analysis of circadian rhythmic transcripts.

Cluster analysis of 412 candidate genes was performed using ClustVis (*https://biit.cs.ut.ee/clustvis/*)(Metsalu & Vilo, 2015). Expression levels were normalized using Min-Max normalization. Green bar indicates Cluster 1; orange bar indicates Cluster 2.

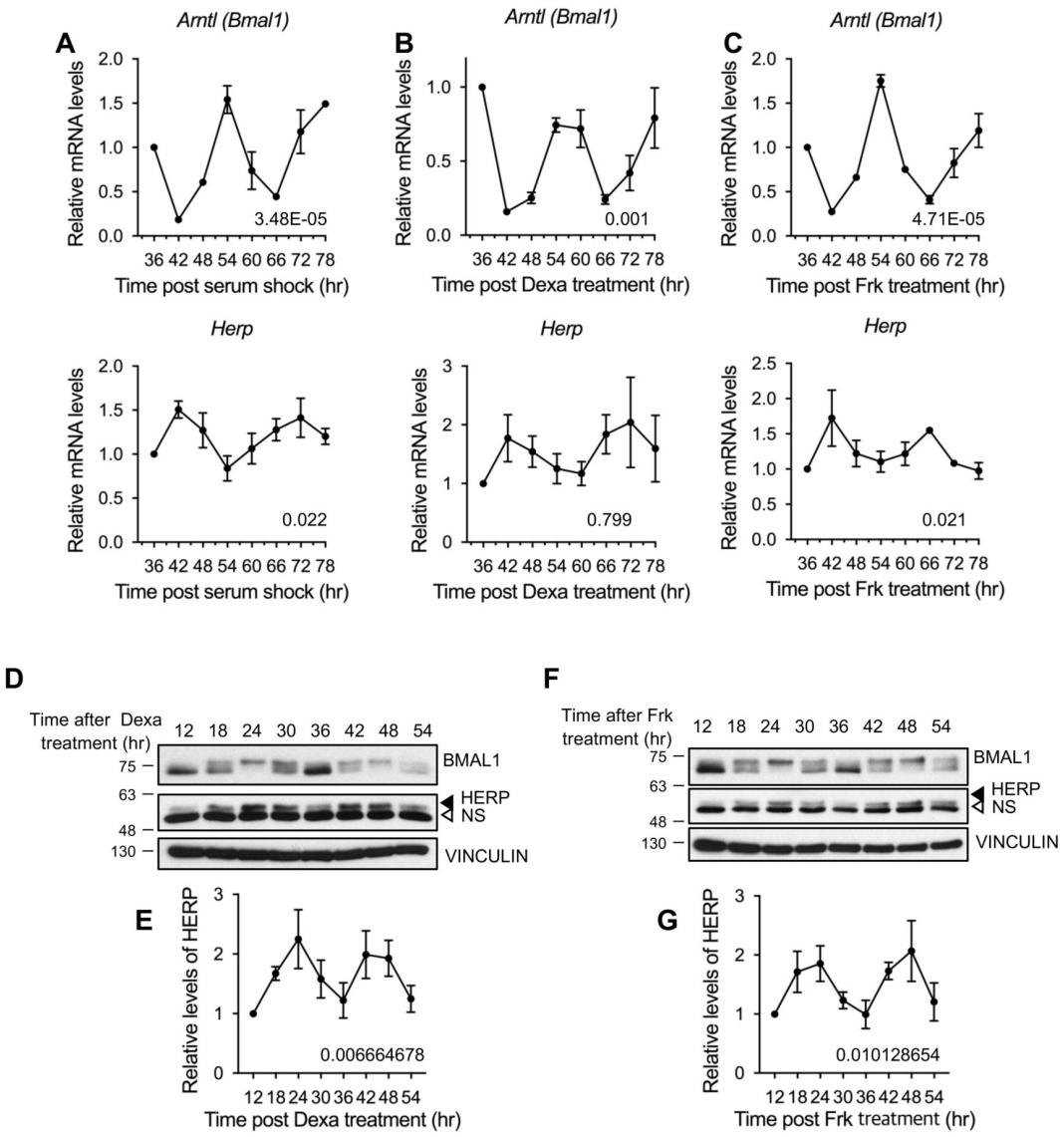

Figure 2-figure supplement 1.

Herp is rhythmically expressed in mouse cultured astrocytes synchronized by forskolin or dexamethasone.

Astrocytes were synchronized using 50% horse serum (A), 100 nM dexamethasone (B, D-E), or 10 μM forskolin (C, F-G), and harvested at the indicated times. (A-C) Real-time qRT-PCR was performed to examine mRNA levels of the indicated genes (D-G) Western blot analysis for BMAL1 and HERP was conducted, with VINCULIN as a loading control. HERP/VINCULIN values at different times were normalized to those at 12hrs post-shock (set to 1). (D, F) Representative Western blot images from three independent experiments. (E, G) Densitometric quantification of Western blots. Rhythmicity was analyzed using MetaCycle. Meta2d *p* values are indicated by insets in graphs. Values are mean ± SEM (n = 3); *p*-values are indicated in the graph insets.

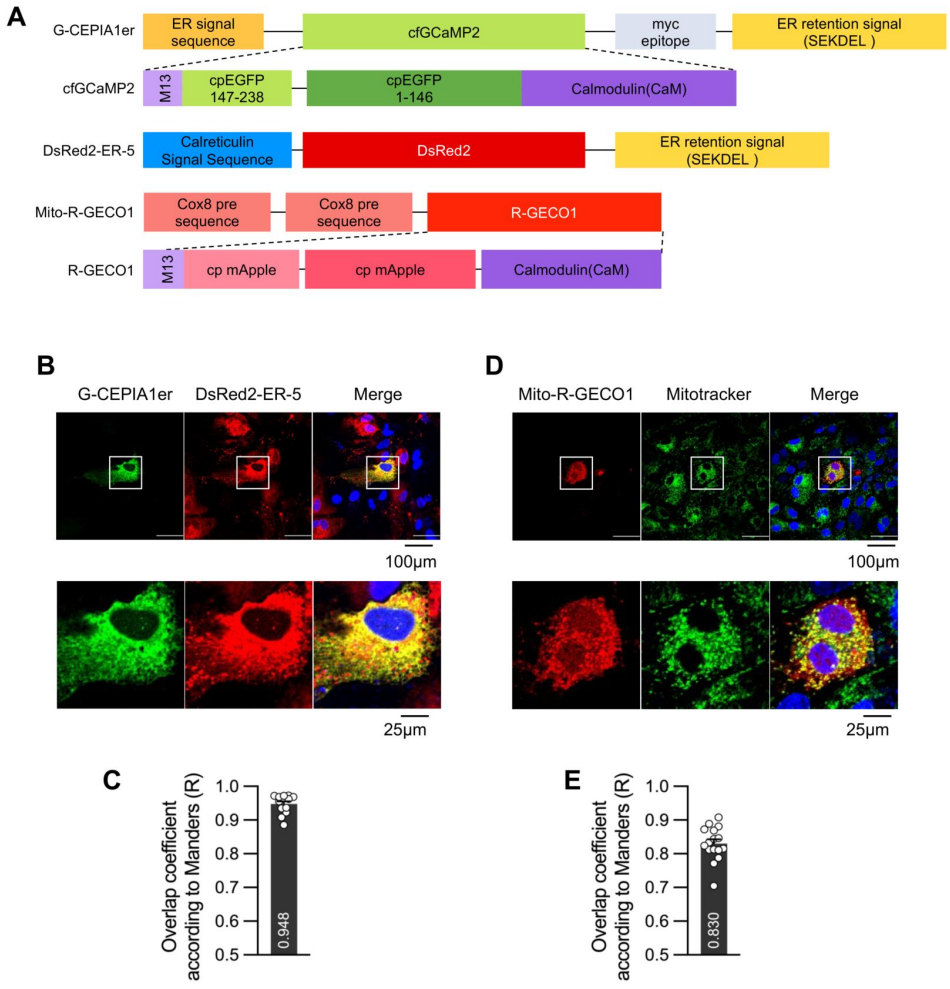

Figure 3-figure supplement 1.

Co-localization of organelle-specific Ca^{2+} sensors with organelle markers.

(A) Schematic diagram showing organelle-specific Ca^{2+} sensors and DsRed2-ER-5. Astrocytes were transfected with Ca^{2+} sensors specific for G-CEPIA1er (B, C) or mito-R-GECO1 (D, E). (B, C) G-CEPIA1er was co-transfected with DsRed2-ER-5 containing calreticulin signal sequence. Live-cell imaging was performed 48hrs post transfection. (D, E) Mito-R-GECO1 was transfected, and live-cell imaging was performed 48hrs post transfection. Before imaging, 200nM Mitotracker was applied for 30 minutes to stain the mitochondria. (C, E) The overlap coefficient (Manders' R value) was calculated from the images. (B, C) n = 13; (D, E) n = 16

Figure 3-figure supplement 2.

Expression profiles of Itpr1, Itpr2 and Itpr3 in cultured astrocytes from RNA-seq data.

White and gray backgrounds represent subjective day and subjective night, respectively.

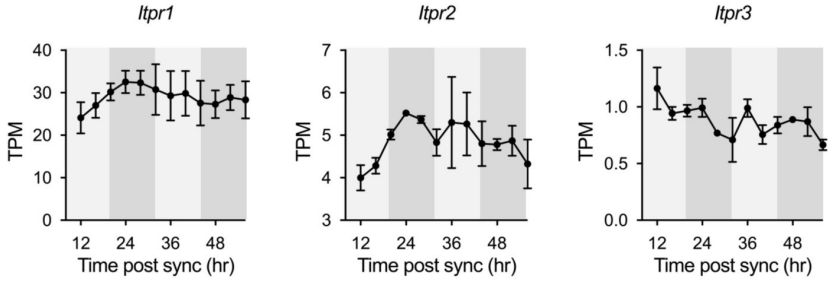

Figure 6-figure supplement 1.

Expression profiles of Cx43 and Cx30 in cultured astrocytes from RNA-seq data.

White and gray backgrounds represent subjective day and subjective night, respectively.

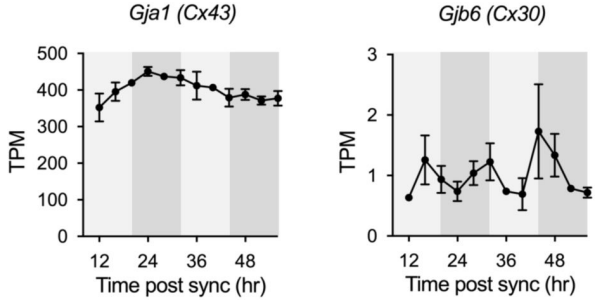

References

Agostinelli F., Ceglia N., Shahbaba B., Sassone-Corsi P., Baldi P (2016) **What time is it? Deep learning approaches for circadian rhythms** *Bioinformatics* **32**:i8–i17 https://doi.org/10.1093/bioinformatics/btw243

Agulhon C., Petravicz J., McMullen A. B., Sweger E. J., Minton S. K., Taves S. R., Casper K. B., Fiacco T. A., McCarthy K. D (2008) **What Is the Role of Astrocyte Calcium in Neurophysiology?** *Neuron* **59**:932–946 https://doi.org/10.1016/j.neuron.2008.09.004

Annayev Y., Adar S., Chiou Y. Y., Lieb J. D., Sancar A., Ye R (2014) **Gene model 129 (Gm129) encodes a novel transcriptional repressor that modulates circadian gene expression** *J Biol Chem* **289**:5013–5024 https://doi.org/10.1074/jbc.M113.534651

Balsalobre A., Brown S. A., Marcacci L., Tronche F., Kellendonk C., Reichardt H. M., Schütz G., Schibler U (2000) **Resetting of circadian time in peripheral tissues by glucocorticoid signaling** *Science* **289**:2344–2347 https://doi.org/10.1126/science.289.5488.2344

Balsalobre A., Damiola F., Schibler U (1998) **A serum shock induces circadian gene expression in mammalian tissue culture cells** *Cell* **93**:929–937 https://doi.org/10.1016/s0092-8674(00)81199-x

Barca-Mayo O., Boender A. J., Armirotti A., De Pietri Tonelli D. (2020) **Deletion of astrocytic BMAL1 results in metabolic imbalance and shorter lifespan in mice** *Glia* **68**:1131–1147 https://doi.org/10.1002/glia.23764

Barca-Mayo O., Pons-Espinal M., Follert P., Armirotti A., Berdondini L., De Pietri Tonelli D. (2017) **Astrocyte deletion of Bmal1 alters daily locomotor activity and cognitive functions via GABA signalling** *Nat Commun* **8** https://doi.org/10.1038/ncomms14336

Baryshnikov S. G., Rogachevskaja O. A., Kolesnikov S. S (2003) **Calcium signaling mediated by P2Y receptors in mouse taste cells** *J Neurophysiol* **90**:3283–3294 https://doi.org/10.1152/jn.00312.2003

Bell-Pedersen D., Cassone V. M., Earnest D. J., Golden S. S., Hardin P. E., Thomas T. L., Zoran M. J (2005) **Circadian rhythms from multiple oscillators: lessons from diverse organisms** *Nat Rev Genet* **6**:544–556 https://doi.org/10.1038/nrg1633

Blum I. D. *et al.* (2021) **Astroglial Calcium Signaling Encodes Sleep Need in Drosophila** *Curr Biol* **31**:150–162 https://doi.org/10.1016/j.cub.2020.10.012

Bojarskaite L. *et al.* (2020) **Astrocytic Ca(2+) signaling is reduced during sleep and is involved in the regulation of slow wave sleep** *Nat Commun* **11** https://doi.org/10.1038/s41467-020-17062-2

Brancaccio M., Edwards M. D., Patton A. P., Smyllie N. J., Chesham J. E., Maywood E. S., Hastings M. H (2019) **Cell-autonomous clock of astrocytes drives circadian behavior in mammals** *Science* **363**:187–192 https://doi.org/10.1126/science.aat4104

Brancaccio M., Patton A. P., Chesham J. E., Maywood E. S., Hastings M. H (2017) **Astrocytes Control Circadian Timekeeping in the Suprachiasmatic Nucleus via Glutamatergic Signaling** *Neuron* **93**:1420–1435 https://doi.org/10.1016/j.neuron.2017.02.030

Brandebura A. N., Paumier A., Onur T. S., Allen N. J (2023) **Astrocyte contribution to dysfunction, risk and progression in neurodegenerative disorders** *Nature Reviews Neuroscience* **24**:23–39 https://doi.org/10.1038/s41583-022-00641-1

Bunger M. K., Wilsbacher L. D., Moran S. M., Clendenin C., Radcliffe L. A., Hogenesch J. B., Simon M. C., Takahashi J. S., Bradfield C. A (2000) **Mop3 is an essential component of the master circadian pacemaker in mammals** *Cell* **103**:1009–1017 https://doi.org/10.1016/s0092-8674(00)00205-1

Carreras-Sureda A., Pihán P., Hetz C (2018) **Calcium signaling at the endoplasmic reticulum: fine-tuning stress responses** *Cell Calcium* **70**:24–31 https://doi.org/10.1016/j.ceca.2017.08.004

Choi D. J., Eun J. H., Kim B. G., Jou I., Park S. M., Joe E. H (2018) **A Parkinson's disease gene, DJ-1, repairs brain injury through Sox9 stabilization and astrogliosis** *Glia* **66**:445–458 https://doi.org/10.1002/glia.23258

Day R. N., Davidson M. W (2009) **The fluorescent protein palette: tools for cellular imaging** *Chem Soc Rev* **38**:2887–2921 https://doi.org/10.1039/b901966a

Dobin A., Davis C. A., Schlesinger F., Drenkow J., Zaleski C., Jha S., Batut P., Chaisson M., Gingeras T. R (2013) **STAR: ultrafast universal RNA-seq aligner** *Bioinformatics* **29**:15–21 https://doi.org/10.1093/bioinformatics/bts635

Enkvist M. O., McCarthy K. D (1992) **Activation of protein kinase C blocks astroglial gap junction communication and inhibits the spread of calcium waves** *J Neurochem* **59**:519–526 https://doi.org/10.1111/j.1471-4159.1992.tb09401.x

Fujii Y., Maekawa S., Morita M (2017) **Astrocyte calcium waves propagate proximally by gap junction and distally by extracellular diffusion of ATP released from volume-regulated anion channels** *Scientific Reports* **7** https://doi.org/10.1038/s41598-017-13243-0

Giaume C., Naus C. C., Sáez J. C., Leybaert L (2021) **Glial Connexins and Pannexins in the Healthy and Diseased Brain** *Physiol Rev* **101**:93–145 https://doi.org/10.1152/physrev.00043.2018

Giorgi C., Marchi S., Pinton P (2018) **The machineries, regulation and cellular functions of mitochondrial calcium** *Nature Reviews Molecular Cell Biology* **19**:713–730 https://doi.org/10.1038/s41580-018-0052-8

Glynn E. F., Chen J., Mushegian A. R (2006) **Detecting periodic patterns in unevenly spaced gene expression time series using Lomb-Scargle periodograms** *Bioinformatics* **22**:310–316 https://doi.org/10.1093/bioinformatics/bti789

Griffin P. *et al.* (2019) **Circadian clock protein Rev-erbalpha regulates neuroinflammation** *Proc Natl Acad Sci U S A* **116**:5102–5107 https://doi.org/10.1073/pnas.1812405116

Guerra-Gomes S., Sousa N., Pinto L., Oliveira J. F (2017) **Functional Roles of Astrocyte Calcium Elevations: From Synapses to Behavior** *Front Cell Neurosci* **11** https://doi.org/10.3389/fncel.2017.00427

Hong H. K., Maury E., Ramsey K. M., Perelis M., Marcheva B., Omura C., Kobayashi Y., Guttridge D. C., Barish G. D., Bass J (2018) **Requirement for NF-κB in maintenance of molecular and behavioral circadian rhythms in mice** *Genes Dev* **32**:1367–1379 https://doi.org/10.1101/gad.319228.118

Hughes M. E., Hogenesch J. B., Kornacker K (2010) **JTK_CYCLE: an efficient nonparametric algorithm for detecting rhythmic components in genome-scale data sets** *J Biol Rhythms* **25**:372–380 https://doi.org/10.1177/0748730410379711

Ingiosi A. M., Hayworth C. R., Harvey D. O., Singletary K. G., Rempe M. J., Wisor J. P., Frank M. G (2020) **A Role for Astroglial Calcium in Mammalian Sleep and Sleep Regulation** *Curr Biol* **30**:4373–4383 https://doi.org/10.1016/j.cub.2020.08.052

James G., Butt A. M (2001) **P2X and P2Y purinoreceptors mediate ATP-evoked calcium signalling in optic nerve glia in situ** *Cell Calcium* **30**:251–259 https://doi.org/10.1054/ceca.2001.0232

Kokame K., Agarwala K. L., Kato H., Miyata T (2000) **Herp, a new ubiquitin-like membrane protein induced by endoplasmic reticulum stress** *J Biol Chem* **275**:32846–32853 https://doi.org/10.1074/jbc.M002063200

Kokame K., Kato H., Miyata T (1996) **Homocysteine-respondent genes in vascular endothelial cells identified by differential display analysis. GRP78/BiP and novel genes** *J Biol Chem* **271**:29659–29665 https://doi.org/10.1074/jbc.271.47.29659

Kunzelmann P., Schroder W., Traub O., Steinhauser C., Dermietzel R., Willecke K (1999) **Late onset and increasing expression of the gap junction protein connexin30 in adult murine brain and long-term cultured astrocytes** *Glia* **25**:111–119 https://doi.org/10.1002/(sici)1098-1136(19990115)25:2<111::aid-glia2>3.0.co;2-i

Lananna B. V., Musiek E. S (2020) **The wrinkling of time: Aging, inflammation, oxidative stress, and the circadian clock in neurodegeneration** *Neurobiol Dis* **139** https://doi.org/10.1016/j.nbd.2020.104832

Lananna B. V. *et al.* (2018) **Cell-Autonomous Regulation of Astrocyte Activation by the Circadian Clock Protein BMAL1** *Cell Rep* **25**:1–9 https://doi.org/10.1016/j.celrep.2018.09.015

Langer J., Stephan J., Theis M., Rose C. R (2012) **Gap junctions mediate intercellular spread of sodium between hippocampal astrocytes in situ** *Glia* **60**:239–252 https://doi.org/10.1002/glia.21259

Leitman J., Shenkman M., Gofman Y., Shtern N. O., Ben-Tal N., Hendershot L. M., Lederkremer G. Z (2014) **Herp coordinates compartmentalization and recruitment of HRD1 and misfolded proteins for ERAD** *Mol Biol Cell* **25**:1050–1060 https://doi.org/10.1091/mbc.E13-06-0350

Marpegan L., Krall T. J., Herzog E. D (2009) **Vasoactive intestinal polypeptide entrains circadian rhythms in astrocytes** *J Biol Rhythms* **24**:135–143 https://doi.org/10.1177/0748730409332042

Mei W., Jiang Z., Chen Y., Chen L., Sancar A., Jiang Y (2020) **Genome-wide circadian rhythm detection methods: systematic evaluations and practical guidelines** *Briefings in Bioinformatics* **22** https://doi.org/10.1093/bib/bbaa135

Metsalu T., Vilo J (2015) **ClustVis: a web tool for visualizing clustering of multivariate data using Principal Component Analysis and heatmap** *Nucleic Acids Res* **43**:W566–570 https://doi.org/10.1093/nar/gkv468

Mohawk J. A., Green C. B., Takahashi J. S (2012) **Central and peripheral circadian clocks in mammals** *Annu Rev Neurosci* **35**:445–462 https://doi.org/10.1146/annurev-neuro-060909-153128

Mure L. S. *et al.* (2018) **Diurnal transcriptome atlas of a primate across major neural and peripheral tissues** *Science* **359** https://doi.org/10.1126/science.aao0318

Nagy J. I., Patel D., Ochalski P. A., Stelmack G. L (1999) **Connexin30 in rodent, cat and human brain: selective expression in gray matter astrocytes, co-localization with connexin43 at gap junctions and late developmental appearance** *Neuroscience* **88**:447–468 https://doi.org/10.1016/s0306-4522(98)00191-2

Neary J. T., van Breemen C., Forster E., Norenberg L. O., Norenberg M. D. (1988) **ATP stimulates calcium influx in primary astrocyte cultures** *Biochem Biophys Res Commun* **157**:1410–1416 https://doi.org/10.1016/s0006-291x(88)81032-5

Nimlamool W., Andrews R. M., Falk M. M (2015) **Connexin43 phosphorylation by PKC and MAPK signals VEGF-mediated gap junction internalization** *Mol Biol Cell* **26**:2755–2768 https://doi.org/10.1091/mbc.E14-06-1105

Oki S., Ohta T., Shioi G., Hatanaka H., Ogasawara O., Okuda Y., Kawaji H., Nakaki R., Sese J., Meno C (2018) **ChIP-Atlas: a data-mining suite powered by full integration of public ChIP-seq data** *EMBO reports* **19** https://doi.org/10.15252/embr.201846255

Pacholko A. G., Wotton C. A., Bekar L. K (2020) **Astrocytes—The Ultimate Effectors of Long-Range Neuromodulatory Networks? [Review]** *Frontiers in Cellular Neuroscience* **14** https://doi.org/10.3389/fncel.2020.581075

Panda S., Antoch M. P., Miller B. H., Su A. I., Schook A. B., Straume M., Schultz P. G., Kay S. A., Takahashi J. S., Hogenesch J. B (2002) **Coordinated transcription of key pathways in the mouse by the circadian clock** *Cell* **109**:307–320 https://doi.org/10.1016/s0092-8674(02)00722-5

Paredes F. *et al.* (2016) **HERPUD1 protects against oxidative stress-induced apoptosis through downregulation of the inositol 1,4,5-trisphosphate receptor** *Free Radic Biol Med* **90**:206–218 https://doi.org/10.1016/j.freeradbiomed.2015.11.024

Patton A. P., Smyllie N. J., Chesham J. E., Hastings M. H (2022) **Astrocytes sustain circadian oscillation and bidirectionally determine circadian period, but do not regulate circadian phase in the suprachiasmatic nucleus** *J Neurosci* **42**:5522–5537 https://doi.org/10.1523/jneurosci.2337-21.2022

Phatnani H., Maniatis T (2015) **Astrocytes in neurodegenerative disease** *Cold Spring Harb Perspect Biol* **7** https://doi.org/10.1101/cshperspect.a020628

Prolo L. M., Takahashi J. S., Herzog E. D (2005) **Circadian Rhythm Generation and Entrainment in Astrocytes** *The Journal of Neuroscience* **25**:404–408 https://doi.org/10.1523/jneurosci.4133-04.2005

Rakshit K., Qian J., Ernst J., Matveyenko A. V (2016) **Circadian variation of the pancreatic islet transcriptome** *Physiological Genomics* **48**:677–687 https://doi.org/10.1152/physiolgenomics.00019.2016

Reddy A. B. *et al.* (2006) **Circadian orchestration of the hepatic proteome** *Curr Biol* **16**:1107–1115 https://doi.org/10.1016/j.cub.2006.04.026

Reinke H., Asher G (2019) **Crosstalk between metabolism and circadian clocks** *Nat Rev Mol Cell Biol* **20**:227–241 https://doi.org/10.1038/s41580-018-0096-9

Schultz T. F., Kay S. A (2003) **Circadian clocks in daily and seasonal control of development** *Science* **301**:326–328 https://doi.org/10.1126/science.1085935

Sofroniew M. V., Vinters H. V (2010) **Astrocytes: biology and pathology** *Acta Neuropathol* **119**:7–35 https://doi.org/10.1007/s00401-009-0619-8

Solan J. L., Lampe P. D (2014) **Specific Cx43 phosphorylation events regulate gap junction turnover in vivo** *FEBS Lett* **588**:1423–1429 https://doi.org/10.1016/j.febslet.2014.01.049

Suzuki J., Kanemaru K., Ishii K., Ohkura M., Okubo Y., Iino M (2014) **Imaging intraorganellar Ca2+ at subcellular resolution using CEPIA** *Nat Commun* **5** https://doi.org/10.1038/ncomms5153

Szabó Z. *et al.* (2017) **Extensive astrocyte synchronization advances neuronal coupling in slow wave activity in vivo** *Scientific Reports* **7** https://doi.org/10.1038/s41598-017-06073-7

Takahashi J. S (2017) **Transcriptional architecture of the mammalian circadian clock** *Nat Rev Genet* **18**:164–179 https://doi.org/10.1038/nrg.2016.150

Torrealba N. *et al.* (2017) **Herpud1 negatively regulates pathological cardiac hypertrophy by inducing IP3 receptor degradation** *Sci Rep* **7** https://doi.org/10.1038/s41598-017-13797-z

Tso C. F., Simon T., Greenlaw A. C., Puri T., Mieda M., Herzog E. D (2017) **Astrocytes Regulate Daily Rhythms in the Suprachiasmatic Nucleus and Behavior** *Current Biology* **27**:1055–1061 https://doi.org/10.1016/j.cub.2017.02.037

Tsunematsu T., Sakata S., Sanagi T., Tanaka K. F., Matsui K (2021) **Region-specific and state-dependent astrocyte Ca2+ dynamics during the sleep-wake cycle in mice. The Journal of Neuroscience** *JN-RM* :2912–2920 https://doi.org/10.1523/jneurosci.2912-20.2021

Verkhratsky A., Nedergaard M (2018) **Physiology of Astroglia** *Physiol Rev* **98**:239–389 https://doi.org/10.1152/physrev.00042.2016

Vyazovskiy V. V., Olcese U., Lazimy Y. M., Faraguna U., Esser S. K., Williams J. C., Cirelli C., Tononi G (2009) **Cortical firing and sleep homeostasis** *Neuron* **63**:865–878 https://doi.org/10.1016/j.neuron.2009.08.024

Wen S., Ma D., Zhao M., Xie L., Wu Q., Gou L., Zhu C., Fan Y., Wang H., Yan J (2020) **Spatiotemporal single-cell analysis of gene expression in the mouse suprachiasmatic nucleus** *Nat Neurosci* **23**:456–467 https://doi.org/10.1038/s41593-020-0586-x

Wu G., Anafi R. C., Hughes M. E., Kornacker K., Hogenesch J. B (2016) **MetaCycle: an integrated R package to evaluate periodicity in large scale data** *Bioinformatics* **32**:3351–3353 https://doi.org/10.1093/bioinformatics/btw405

Wu J. *et al.* (2013) **Improved orange and red Ca²± indicators and photophysical considerations for optogenetic applications** *ACS Chem Neurosci* **4**:963–972 https://doi.org/10.1021/cn400012b

Yagita K., Okamura H (2000) **Forskolin induces circadian gene expression of rPer1, rPer2 and dbp in mammalian rat-1 fibroblasts** *FEBS Lett* **465**:79–82 https://doi.org/10.1016/s0014-5793(99)01724-x

Yang R., Su Z (2010) **Analyzing circadian expression data by harmonic regression based on autoregressive spectral estimation** *Bioinformatics* **26**:i168–174 https://doi.org/10.1093/bioinformatics/btq189

Yoo S. H., Ko C. H., Lowrey P. L., Buhr E. D., Song E. J., Chang S., Yoo O. J., Yamazaki S., Lee C., Takahashi J. S (2005) **A noncanonical E-box enhancer drives mouse Period2 circadian oscillations in vivo** *Proc Natl Acad Sci U S A* **102**:2608–2613 https://doi.org/10.1073/pnas.0409763102

Yoshitane H., Takao T., Satomi Y., Du N. H., Okano T., Fukada Y (2009) **Roles of CLOCK phosphorylation in suppression of E-box-dependent transcription** *Mol Cell Biol* **29**:3675–3686 https://doi.org/10.1128/mcb.01864-08

Zhang R., Lahens N. F., Ballance H. I., Hughes M. E., Hogenesch J. B (2014) **A circadian gene expression atlas in mammals: implications for biology and medicine** *Proc Natl Acad Sci U S A* **111**:16219–16224 https://doi.org/10.1073/pnas.1408886111

Zhang X., Patel S. P., McCarthy J. J., Rabchevsky A. G., Goldhamer D. J., Esser K. A (2011) **A non-canonical E-box within the MyoD core enhancer is necessary for circadian expression in skeletal muscle** *Nucleic Acids Research* **40**:3419–3430 https://doi.org/10.1093/nar/gkr1297

Zhao Y. *et al.* (2011) **An expanded palette of genetically encoded Ca²⁺ indicators** *Science* **333**:1888–1891 https://doi.org/10.1126/science.1208592

Zou Z., Ohta T., Miura F., Oki S (2022) **ChIP-Atlas 2021 update: a data-mining suite for exploring epigenomic landscapes by fully integrating ChIP-seq, ATAC-seq and Bisulfite-seq data** *Nucleic Acids Research* **50**:W175–W182 https://doi.org/10.1093/nar/gkac199

Metsalu T., Vilo J (2015) **ClustVis: a web tool for visualizing clustering of multivariate data using Principal Component Analysis and heatmap** *Nucleic Acids Res* **43**:W566–570 https://doi.org/10.1093/nar/gkv468

Author information

Ji Eun Ryu[†]
Neuroscience Graduate Program, Department of Biomedical Sciences, Ajou University Graduate School of Medicine, Suwon, Republic of Korea, Department of Brain Science, Ajou University School of Medicine, Suwon, Republic of Korea
ORCID iD: 0009-0000-1438-5018

[†]These authors contributed equally.

Kyu-Won Shim[†]
Interdisciplinary Program in Bioinformatics, Seoul National University, Seoul, Republic of Korea

[†]These authors contributed equally.

Hyun Woong Roh[†]
Neuroscience Graduate Program, Department of Biomedical Sciences, Ajou University Graduate School of Medicine, Suwon, Republic of Korea, Department of Psychiatry, Ajou University School of Medicine, Suwon, Republic of Korea

[†]These authors contributed equally.

Minsung Park
Neuroscience Graduate Program, Department of Biomedical Sciences, Ajou University Graduate School of Medicine, Suwon, Republic of Korea, Department of Brain Science, Ajou University School of Medicine, Suwon, Republic of Korea

Jae-Hyung Lee
Department of Oral Microbiology, College of Dentistry, Kyung Hee University, Seoul, Republic of Korea
ORCID iD: 0000-0002-5085-6988

For correspondence: jaehlee@khu.ac.kr

Eun Young Kim
Neuroscience Graduate Program, Department of Biomedical Sciences, Ajou University Graduate School of Medicine, Suwon, Republic of Korea, Department of Brain Science, Ajou University School of Medicine, Suwon, Republic of Korea

For correspondence: ekim@ajou.ac.kr

Editors

Reviewing Editor
Annalisa Scimemi
University at Albany, State University of New York, Albany, United States of America

Senior Editor
Sacha Nelson
Brandeis University, Waltham, United States of America

Reviewer #2 (Public review):

Summary:

The article by Ryu and colleagues describes the circadian control of astrocytic intracellular calcium levels in vitro.

Strengths:

The authors used a variety of technical approaches that are appropriate and considerably improved the manuscript with experiments and more solid data analysis compared to the first version

Weaknesses:

Some conceptual issues are still present. This is a mechanistic paper done completely in vitro, all references to the in vivo situation are speculative and should be absolutely avoided unless the authors are citing in vivo work.

https://doi.org/10.7554/eLife.96357.2.sa2

Reviewer #3 (Public review):

This study provides significant insights into how the circadian clock influences astrocytic Ca2+ homeostasis. Astrocyte biology is an active area of research and this study is timely and adds to a growing body of literature in the field. This research highlights the potential importance of circadian rhythms in astrocytes, offering a new perspective on their role in central nervous system regulation.

https://doi.org/10.7554/eLife.96357.2.sa1

Author response:

The following is the authors' response to the original reviews.

> ***Public Reviews:***
>
> ***Reviewer #1 (Public Review):***
>
> *Summary:*
>
> *In Ryu et al., the authors use a cortical mouse astrocyte culture system to address the functional contribution of astrocytes to circadian rhythms in the brain. The authors' starting point is transcriptional output from serum-shocked culture, comparative informatics with existing tools and existing datasets. After fairly routine pathway analyses, they focus on the calcium homeostasis machinery and one gene, Herp, in particular. They argue that Herp is rhythmic at both mRNA and protein levels in astrocytes. They then use a calcium reporter targeted to the ER, mitochondria, or cytosol and show that Herp modulates calcium signaling as a function of circadian time. They argue that this occurs through the regulation of inositol receptors. They claim that the signaling pathway is clock-controlled by a limited examination of Bmal1 knockout astrocytes. Finally, they switch to calcium-mediated phosphorylation of the gap junction protein Connexin 43 but do not directly connect HERP-mediated circadian signaling to these observations. While these experiments address very important questions related to the critical role of astrocytes in regulating circadian signaling, the mechanistic arguments for HERP function, its role in circadian signaling through inositol receptors, the connection to gap junctions, and ultimately, the functional relevance of these findings is only partially substantiated by experimental evidence.*
>
> *Strengths:*
>
> *- The paper provides useful datasets of astrocyte gene expression in circadian time.*
>
> *- Identifies HERP as a rhythmic output of the circadian clock.*

> *- Demonstrates the circadian-specific sensitivity of ATP -> calcium signaling.*
>
> *- Identifies possible rhythms in both Connexin 43 phosphorylation and rhythmic movement of calcium between cells.*
>
> *Weaknesses:*
>
> *- It is not immediately clear why the authors chose to focus on Ca2+ homeostasis or Herp from their initial screens as neither were the "most rhythmic" pathways in their primary analyses.*

We appreciate the reviewer's comment. We chose to focus on Ca2+ homeostasis processes because intracellular Ca2+ signaling plays crucial role in numerous astrocyte functions and is notably associated with sleep/wake status of animals, which is our primary interest (Bojarskaite et al., 2020; Ingiosi et al., 2020; Blum et al., 2021; Szabó et al., 2017). Among the genes involved in calcium ion homeostasis, Herp exhibited the most robust rhythmicity (supplementary table 1). The rationale for our focus on Ca2+ homeostasis and Herp is explained in the results section (line 143-150). We hope this provides a clear justification for our focus.

> *- It would have been interesting (and potentially important) to know whether various methods of cellular synchronization would also render HERP rhythmic (e.g., temperature, forskolin, etc). If Herp is indeed relatively astrocyte-specific and rhythmic, it should be easy to assess its rhythmicity in vivo.*

Thank you for the reviewer's insightful comment. In response, we examined HERP expression in cultured astrocytes synchronized using either Dexamethasone or Forskolin treatment. We found that Herp exhibited rhythmic expression at both the the mRNA and protein levels under these conditions. These results have been added to Figure S3 and are explained in the manuscript (lines 173-175).

Additionally, we measured HERP levels in the prefrontal cortex of mice at CT58 and CT70 and found no rhythmicity, as shown in Author response image 1. Given that Herp is expressed in various brain cell types, including microglia, endothelial cells, neurons, oligodendrocytes, and the astrocytes- with the highest expression in microglia(Cahoy et al., 2008), we reason that the potential rhythmic expression of HERP in astrocytes might be masked by its continuous expression in other cell types. Nonetheless, to assess HERP rhythmicity specifically in astrocytes in vivo, we attempted immunostaining using several anti-HERP antibodies, but none were successful. Consequently, we were unable to determine whether HERP exhibits rhythmic expression in astrocytes in vivo.

Author response image 1.

HERP levels were constant at CT58 and CT70. (A, B) Mice were entrained under 12h:12h LD cycle and maintained in constant dark. Prefrontal cortices were harvested at indicated time and processed for Western blot analysis. Representative image shows three independent samples. (B) Quantification of HERP levels normalized to VINCULIN. Values in graphs are mean ± SEM (*p < 0.05, **p < 0.005, ***p < 0.0005, and ****p < 0.00005; t-test)

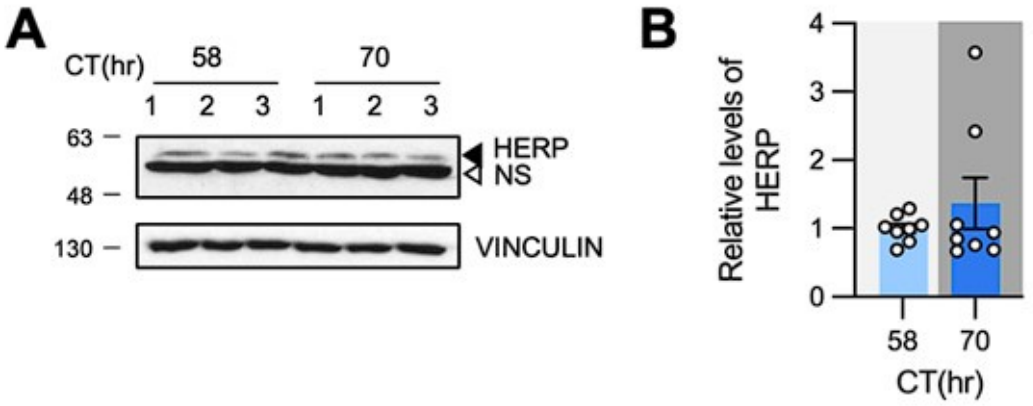

> *- The authors show that Herp suppression reduces ATP-mediated suppression of calcium whereas it initially increases Ca2+ in the cytosol and mitochondria and then suppresses it. The dynamics of the mitochondrial and cytosolic responses are not discussed in any detail and it is unclear what their direct relationship is to Herp-mediated ER signaling. What is the explanation for Herp (which is thought to be ER-specific) to calcium signaling in other organelles?*

Our examination of cytosolic and mitochondrial Ca2+ responses was aimed at corroborating HERP's effect on ER Ca2+ response. Upon ATP stimulation, Ca2+ is released from the ER via IP3R receptors (IP3Rs) and subsequently transmitted to other organelles including mitochondria (Carreras-Sureda et al., 2018; Giorgi et al., 2018). Ca2+ is directly transferred to the cytosol by IP3Rs located on the ER membrane, and to the mitochondria through a complex formed by IP3R and the voltage-dependent anion channel (VDAC) on the mitochondria (Giorgi et al., 2018). Consistent with previous reports, we observed an increase of cytosolic and mitochondrial Ca2+ levels accompanied by decrease in ER Ca2+ levels following ATP treatment (See Fig. 3B, E, H, control siRNA). The ATP-stimulated ER Ca2+ release was enhanced by Herp knockdown. We reasoned that if Ca2+ release was enhanced, then cytosolic and mitochondrial Ca2+ uptakes would also be enhanced. The results were consistent with our hypothesis (See Fig. 3B, E, H, Herp siRNA). These observations are described in the Results section (lines 202-208) and in the Discussion (lines 333-348). We hope this explanation clarifies the relationship between Herp-mediated ER Ca2+ response and Ca2+ response in other organelles. Thank you for your consideration.

> *- What is the functional significance of promoting ATP-mediated suppression of calcium in ER?*

In astrocytes, intracellular Ca2+ plays crucial role in regulating several processes. In this study, among various downstream effects of intracellular Ca2+, we examined the gap junction channel (GJC) conductance, which affects astrocytic communication. As discussed in the manuscript (lines 357-381), circadian variation in HERP results in rhythmic Cx43 (S368) phosphorylation linked with GJC conductance. We propose that during the subjective night phase, heightened ATP induced ER Ca2+ release reduces GJC conductance, uncoupling astrocytes from the syncytium, making them better equipped for localized response. On the other hand, during the subjective day phase, increased GJC conductance may allow astrocytes to control a larger area for synchronous neuronal activity which is a key feature of sleep.

> *- The authors then nicely show that the effect of ATP is dependent on intrinsic circadian timing but do not explain why these effects are antiphase in cytosol or mitochondria.*

Moreover, the ΔF/F for calcium in mitochondria and cytosol both rise, cross the abscissa, and then diminish - strongly suggesting a biphasic signaling event. Therefore, one wonders whether measuring the area under the curve is the most functionally relevant measurement of the change.

We appreciate the reviewer's insightful comments. As explained in our previous response, Ca2+ released from the ER is transferred to the cytosol and mitochondria. This transfer explains why the fluorescent intensities of cytosolic and mitochondrial Ca2+ indicators show anti-phasic responses to those of the ER.

We agree that cytosolic and mitochondrial Ca2+ responses may be biphasic. The decrease below the abscissa in mitochondria and cytosol likely reflects Ca2+ extrusion from these organelles. However, our primary focus was on the initial uptake of Ca2+ following ER Ca2+ release. Thus, when calculating the area under the curve (AUC), we measured the area between the ΔF/F graph and the y=0 (X-axis) for both mitochondria and cytosol. We reason that the measuring the area under the curve (above the abscissa) fits with our objective.

While addressing your concerns, we noticed errors in the Y-axis labels of Fig. 3C, 4D, and 5C. For the ER Ca2+ dynamics, we measured the area above curve. These mistakes have now been corrected.

> *- Why are mitochondrial and cytosolic calcium not also demonstrated for Bmal1 KO astrocytes?*

In two sets of experiments (Fig. 3 and Fig. 4), we demonstrated that the increase in cytosolic and mitochondrial Ca2+ aligns with ER Ca2+ release. Since there were no circadian time differences in ER Ca2+ release in the Bmal1 KO cultures, we concluded that it was unnecessary to measure Ca2+ levels in the mitochondria and cytosol. Additionally, our primary focus is on the ER Ca2+ response rather than the Ca2+ dynamics in subcellular organelles. We hope this clarifies our rationale and maintains the focus of our study.

> *- The authors claim that Herp acts by regulating the degradation of ITPRs but this hypothesis - rather central to the mechanisms proposed in this study - is not experimentally substantiated.*

We appreciate the reviewer's insightful comments regarding the role of HERP in the degradation of IP3Rs. In the original manuscript, we demonstrated that treating cells with Herp siRNA leads to an increase in the levels of ITPR1 and ITPR2, suggesting that HERP might be involved in the regulation of IP3Rs stability. This observation is consistent with previous studies, which showed that Herp siRNA treatment increases ITPR levels in HeLa and cardiac cells (Paredes et al., 2016; Torrealba et al., 2017). Torrealba et al. also showed that HERP regulates the polyubiquitination of IP3Rs. Based on our results and previous reports, we hypothesized that HERP similarly regulates ITPR degradation in cultured astrocytes.

However, as the reviewer rightly pointed out, further evidence is needed to confirm that HERP specifically regulates ITPR degradation. To address this, we conducted new experiments examining the effect of XesC, an inhibitor of IP3Rs, on ER Ca2+ release. The treatment of XesC reduced the ER Ca2+ release and abolished the enhancement of ER Ca2+ release by Herp KD. These results demonstrated that HERP influences ER Ca2+ response through IP3Rs. These new findings have been added to Fig. 3N – 3P and explained in the Results section (lines 217-221).

We believe these additional experiments and clarifications strengthen our hypothesis that HERP regulates IP3R degradation, thereby modulating ER Ca2+ responses.

> *- There is no clear demonstration of the functional relevance of the circadian rhythms of ATP-mediated calcium signaling.*

As mentioned in the previous response, we examined Cx43 phosphorylation linked with GJC conductance in the context of ATP-mediated Ca2+ signaling. Our results demonstrated circadian variations in Cx43 Ser368 phosphorylation leading to variations of gap junction channel (GJC) conductance (Fig. 6C – F and Fig. 7D - I). We have discussed the significance of this circadian rhythm in ATP driven ER Ca2+ signaling concerning astrocytic function during sleep/wake states in the manuscript (lines 357 – 382) as follows.

"ATP-stimulated Cx43 (S368) phosphorylation is higher at 30hr (subjective night phase) than at 42hr (subjective day phase) (Fig. 6C and 6D.), a finding further supported by in vivo experiments showing higher pCx43(S368) levels in the prefrontal cortex during the subjective night than during the day (Fig. 6E and 6F). What are the implications of this day/night variation in Cx43 (S368) phosphorylation? We reasoned that the circadian variation in Cx43 phosphorylation could significantly impact astrocyte functionality within the syncytium. Indeed, our cultured astrocytes exhibited circadian phase-dependent variation in gap junctional communication (Fig.7D – 7F). Astrocytes influence synaptic activity through the release of gliotransmitters such as glutamate, GABA, D-serine, and ATP, triggered by increases in intracellular Ca2+ in response to the activity of adjacent neurons and astrocytes (Verkhratsky & Nedergaard, 2018). Importantly, this increase in Ca2+ spreads to adjacent astrocytes through GJCs (Fujii et al., 2017), influencing a large area of the neuronal network. Considering that Cx43 Ser368 phosphorylation occurs to uncouple specific pathways in the astrocytic syncytium to focus local responses (Enkvist & McCarthy, 1992), our findings suggest that astrocytes better equipped for localized responses when presented with a stimulus during the active phase in mice. Conversely, during the rest period, characterized by more synchronous neuronal activity across broad brain areas (Vyazovskiy et al., 2009) higher GJC conductance might allow astrocytes to exert control over a larger area. In support of this idea, recent study showed that synchronized astrocytic Ca2+ activity advances the slow wave activity (SWA) of the brain, a key feature of non-REM sleep (Szabó et al., 2017). Blocking GJC was found to reduce SWA, further supporting this interpretation. However, conflicting findings have also been reported. For instance, Ingiosi et al. (Ingiosi et al., 2020) found that astrocytic synchrony was higher during wakefulness than sleep in the mouse frontal cortex. Whether these differing results in astrocyte synchrony during resting and active periods are attributable to differences in experimental context (e.g., brain regions, sleep-inducing condition) remains unclear. Indeed, astrocyte Ca2+ dynamics during wakefulness/sleep vary according to brain regions (Tsunematsu et al., 2021). While the extent of astrocyte synchrony might differ depending on brain region and/or stimulus, on our results suggest that the baseline state of astrocyte synchrony, which is affected by GJC conductance, varies with the day/night cycle."

> ***Reviewer #2 (Public Review):***
>
> *Summary:*
>
> *The article entitled "Circadian regulation of endoplasmic reticulum calcium response in mouse cultured astrocytes" submitted by Ryu and colleagues describes the circadian control of astrocytic intracellular calcium levels in vitro.*
>
> *Strengths:*
>
> *The authors used a variety of technical approaches that are appropriate*

We appreciate the reviewer's acknowledgement of the strengths of our manuscript.

> *Weaknesses:*
>
> *Statistical analysis is poor and could lead to a misinterpretation of the data*

Thank you for the comment. We have carefully reviewed our statistical analyses and applied appropriate methods where necessary. Please see below for the specific revisions and improvements made.

For Fig. 2D-E, we initially used a *t*-test. However, after adding more replicates and conducting a normality test, we found that the data did not follow a normal distribution. Therefore, we switched to the Mann-Whitney *U* test. In Fig. 5D-E, we originally used a repeated measures two-way ANOVA, but we have now changed it to a standard two-way ANOVA. For Fig. 7C and I, we also observed non-normal distribution in the normality test and consequently replaced the t-test with the Mann-Whitney U test. For other analyses not specifically mentioned, normality tests confirmed normal distribution, allowing us to use t-tests or ANOVA as appropriate for statistical analysis.

> *Several conceptual issues have been identified.*

We have addressed the reviewer's concerns. Please see our detailed point-by-point responses below.

> *Overinterpretation of the data should be avoided. This is a mechanistic paper done completely in vitro, all references to the in vivo situation are speculative and should be avoided.*

We appreciate the reviewer's insightful comment. Following the reviewer's suggestion, we have removed the interpretations of GO pathways in the context of in vivo situation.

> ***Reviewer #3 (Public Review):***
>
> *Astrocyte biology is an active area of research and this study is timely and adds to a growing body of literature in the field. The RNA-seq, Herp expression, and Ca2+ release data across wild-type, Bmal1 knockout, and Herp knockdown cellular models are robust and lend considerable support to the study's conclusions, highlighting their importance. Despite these strengths, the manuscript presents a gap in elucidating the dynamics of HERP and the involvement of ITPR1/2 in modulating Ca2+ release patterns and their circadian variations, which remains insufficiently supported and characterized. While the Connexin data underscore the importance of rhythmic Ca2+ release triggered by ATP, the relationship here appears correlational and the role of HERP and ITPR in Cx function remains to be characterized. Moreover, enhancing the manuscript's clarity and readability could significantly benefit the presentation and comprehension of the findings.*

We appreciate the reviewer's acknowledgement of the strengths of our manuscript. Regarding the identified gaps, we have conducted several new experiments to clearly demonstrate the HERP-ITPR-Cx phosphorylation axis. Please see our detailed point-by-point responses below.

> ***Recommendations for the authors:***
>
> ***Reviewer #1 (Recommendations For The Authors):***
>
> *- While HERP appears to be a clock-controlled gene and its protein levels appear to demonstrate rhythmicity as well, the data quality of the western blotting in Bmal1*

> *knockout raises some concern about the accuracy of HERP protein quantification.*

We understand the reviewer's concern regarding the proximity of the HERP band to a nonspecific band in the Western blotting for the Bmal1 knockout. However, we took great care to ensure the accuracy of our HERP band quantification. We meticulously selected only the specific HERP band, excluding nonspecific band. Therefore, we are confident in the accuracy of our HERP protein measurements.

> *- If HERP is rhythmic and ITPRs are not, if their model is correct, might we expect HERP suppression to result in 'unmasking' an ITPR rhythm?*

Our model suggests that both HERP and ITPRs are rhythmic, with HERP regulating the degradation of ITPR proteins and driving their rhythms. Consistent with this, we observed that day/night variations in ITPR2 levels (Fig. 4N and 4O). Therefore, we concluded that circadian variations in HERP are sufficient to drive ITPR2 rhythms. We have explained this in detail in the Result section (lines 236-241) and the Discussion section (lines 324-332).

> *- The authors make a rather abrupt switch to examining gap junctions and connexin 43 phosphorylation. While the data demonstrating that the phosphorylation of S368 may indeed be rhythmic - the authors do not connect these data to the rest of the manuscript by showing a connection to HERP-mediated calcium signaling, limiting the coherence of the narrative.*

Thank you for the reviewer's insightful comments. To address the reviewer's concern regarding the connection between Herp and the phosphorylation of CX43 at S368, we have conducted new experiments to test whether KD of Herp abolishes the rhythms of Cx43 phosphorylation at S368. We found that the phosphorylation of Cx43 at S368 is significantly enhanced at 30hrs post sync compared with 42hrs post sync in control siRNA-treated astrocytes consistent with our previous results (Fig. 6C & 6D). On the other hand, this circadian phase dependent difference in phosphorylation was abolished in Herp siRNA treated astrocytes. These results clearly indicate that circadian variations in Cx43 phosphorylation are driven by the HERP. These new results are now included in Fig. 6G and 6H and explained in the Results section (lines 276-281).

> *- Comment on data presentation: the authors repeatedly present histograms with attached lines between data points - from my understanding of the experiments, this is inappropriate unless these were repeated measures from the same cells. Otherwise, the lines connecting one data point to another between different conditions (e.g., Ctrl or Herp knockdown) are arbitrary and possibly misleading (i.e., Figure 3K, 3M, 4L, 6D).*

Thank you for the reviewer's comment. We have updated the figures by removing the lines connecting data points in the relevant figures (Fig.3K, M, Fig4.N and Fig.6D)).

> ***Reviewer #2 (Recommendations For The Authors):***
>
> *Most of the suggestions of this reviewer are related to the conceptual interpretation and presentation of the data and to the statistical analysis*
>
> *In Figure 1 the authors analyzed the rhythmic transcriptome of cortical astrocytes synchronized with a serum shock in two different ways. The authors need to discuss what is the difference between the two methods used to detect rhythmic transcripts and make sense of them.*

Following the reviewer's suggestion, we have provided a more detailed explanation about MetaCycle and BioCycle, as well as the rationale for using both packages in our analysis as

follows: “Various methods have been used to identify periodicity in time-series data, such as Lomb-Scargle (Glynn et al., 2006), JTK_CYCLE (Hughes et al., 2010) and ARSER (Yang & Su, 2010), each with distinct advantages and limitations. MetaCycle, integrates these three methods, facilitating the evaluation of periodicity in time-series data without requiring the selection of an optimal algorithm (Wu et al., 2016). Additionally, BioCycle has been developed using a deep neural network trained with extensive synthetic and biological time series datasets (Agostinelli et al., 2016). Because MetaCycle and Biocycle identify periodic signal based on different algorithms, we applied both packages to identify periodicity in our time-series transcriptome data. BioCycle and MetaCycle analyses detected 321 and 311 periodic transcripts, respectively (FDR corrected, q-value < 0.05) (Fig. 1B). Among these, 220 (53.4%) were detected by both methods, but many transcripts did not overlap. MetaCycle is known for its inability to detect asymmetric waveforms (Mei et al., 2020). In our analysis, genes with increasing waveforms like Adora1 and Mybph were identified as rhythmic only by BioCycle, while Plat and Il34 were identified as rhythmic only by MetaCycle (Fig. S1C). Despite these discrepancies, the clear circadian rhythmic expression profiles of these genes led us to conclude that using the union of the two lists compensates for the limitations of each algorithm.”

Please refer to lines 105-117 in the Results section.

> *The reasoning for comparing CT0 with the phase of the clock 8 hs after SS needs to be explained. Circadian time (CT) conceptually refers to the clock phase in the absence of entrainment cues in vivo, the direct transformation of "time after synchronization" in vitro to CT is misleading.*

Thank you for the reviewer’s insightful comments. Initially, we believed that transforming TASS to CT, despite being in vitro data, might provide a more intuitive and physiologically relevant interpretation of our results. However, we agree that this approach might be misleading. Following the reviewer’s suggestion, we have revised our terminology by changing “CT” to “Time post sync (hr)”. Nonetheless, in Fig. 1F for circular peak phase map, we set 8hrs post sync to ZT0 based on a phase comparison result in Fig. 1D for physiologically relevant interpretation. We hope these revisions clarify our approach.

> *Moreover, also by definition a CT cannot be defined in terms of "dark" or "light". Figure 6M needs to be changed.*

Following the reviewer’s suggestion, we removed the labels CT22 and CT34. Instead. we have labeled the respective periods as “30hr post sync” and “42hr post sync”.

> *In Figure 1D, the authors present a gene ontology analysis that is certainly interesting, however, it should not be overinterpreted when trying to explain processes that take place only in vivo (e.g. wound repair).*

Thank you for the insightful comment. Following the reviewer’s feedback, we have removed the paragraph interpreting the cell migration process in relation to wound repair and have focused instead on Ca2+ ion homeostasis.

> *In Figure 2A the relative expression of clock genes and Herp is again misleading by a white/grey shading indicating subjective night and subjective day when the system under study is a cell culture.*

We understand the reviewer’s concern that a cell culture system is not equivalent to light/dark entrainment condition. However, we apply time-synchronizing stimuli to recapitulate in vivo entrainment. In addition, by comparing our data with CircaDB, we

defined 8hrs post sync as corresponding to ZT0, thus aligning it with the beginning of the day. We have retained the shading to facilitate easier interpretation of our data in relation to in vivo situations. However, in response to the reviewer's concern, we have revised the shading from white/grey to light grey/dark grey. We hope this adjustment addresses the reviewer's concern, but if the reviewer still believes it is inappropriate, please let us know, we will gladly update it.

> *In the Figure 2A legend, it is indicated that rhythmicity is assessed using MetaCycle with mean values obtained from n=2. The authors need to make clear whether this n=2 mean: 2 biological replicates or 2 technical replicates. This difference is relevant because it would make the analysis statistically valid or invalid, respectively.*

Thank you for your feedback. n=2 refers to 2 biological replicates. Therefore, the analysis is statistically valid.

> *In Figures 2C and D the authors applied a T-test, a parametric statistical test for one-to-one comparison that requires normality distribution of the data to be tested first. To test normality, the authors need at least 4 biological replicates. The suggestion of this reviewer is that these experiments have to be repeated and proper statistics applied.*

Thank you for your feedback. In response to the reviewer's suggestion, we conducted additional experiments to increase the number of biological replicates to 4. After verifying the normality of the data, we applied a t-test for Figure 2C and a Mann-Whitney test for Figure 2D and 2E. These tests confirmed significant statistical difference between groups.

> *Further evidence of Bmal1-dependent control of HERP circadian expression authors could check the presence of E-Box elements in the Herp promoter.*

Thank you for the reviewer's insightful comment. In the original version of our manuscript's Discussion section, we mentioned the absence of a canonical E-Box in the upstream of Herp gene. However, following the reviewer's suggestion and considering the potential role of non-canonical E-Boxes, we conducted an additional analysis. This analysis identified several non-canonical E-Boxes within the 6 kb upstream region of the Herp gene (Table S2). Notably, we found one non-canonical E-Box, "CACGTT," known to regulate circadian expression (Yoo et al., 2005) is close to the transcription start site (chr8:94386194-94386543). Moreover, this element is evolutionarily conserved across various mammals, including humans, rats, mice, dogs, and opossums (See Author response image 2). Therefore, we reasoned that these non-canonical E boxes might drive the CLOCK/BMAL1 dependent expression of Herp. We have updated the Discussion to reflect these findings in lines 315-319.

Author response image 2.

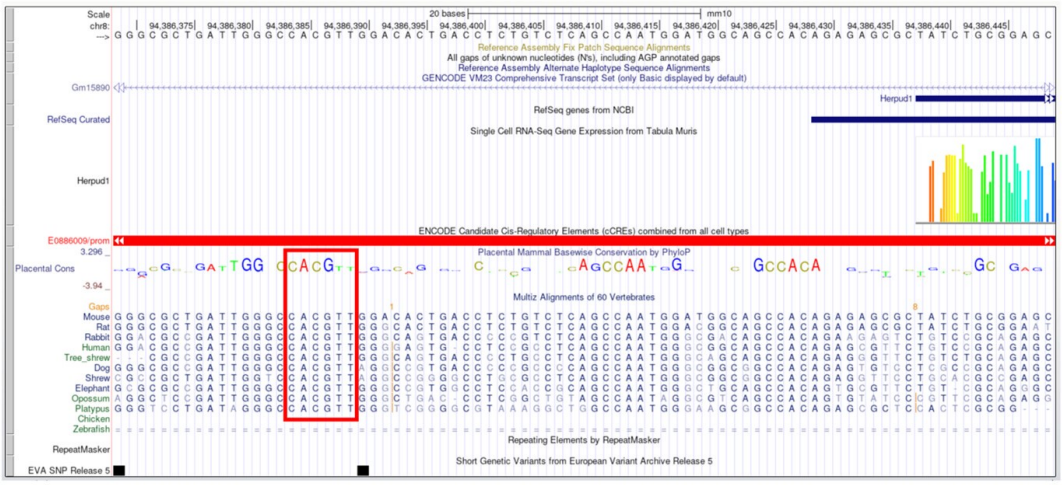

> *The calcium experiments shown in Figures 3A-I, could be more convincing if the authors showed that the different Ca2+ sensors are compartment-specific by showing co-localization with a subcellular marker. In the pictures shown it is not even possible to recognize the cell dimensions.*

Following the reviewer's suggestion, we performed co-staining experiments with organelle specific Ca2+ indicators and organelle markers. First, astrocytes were co-transfected with G-CEPIA1er, an ER specific Ca2+ indicator and ER targeted DsRed2 (with Calreticulin signal sequence). Live imaging analysis showed that the fluorescent intensities of G-CEPIA1er and DsRed2-ER-5 significantly overlapped in co-transfected cells. Secondly, astrocytes were transfected with Mito-R-GECO1 and Mitotracker, a cell permeable mitochondria dye, was applied. The fluorescent intensities of Mito-R-GECO1 and Mitotracker also significantly overlapped. These new data are included in Figure S4 and explained in the Result section (lines 194-195).

> *Data analysis in Figure 3 K and M is misleading. According to the explanations of the results, each of the experiments to assess ITRP1 or 2 is run independently. Then it is not clear why the relative levels obtained with control or Herp siRNA are plotted as pairs. Same comment as above for Figure 4L and Figure 6D.*

Thank you for the reviewer's insightful comments. Reviewer1 raised similar issues. Following the reviewers' suggestions, we have removed the lines connecting the data points in Fig. 3K, 3M, 4L, and 6D.

> *In Figure 5E the authors need to explain why they consider that repeated measures 2-way ANOVA is the right statistical test to apply. According to the explained experimental design, cells transfected, synchronized, and then harvested independently at the indicated time after synchronization.*

Thank you for the reviewer's insightful comment. Upon reviewing the statistical methods as suggested, we have revised our approach. Instead of using repeated measures 2-way ANOVA, we have now applied a standard 2-way ANOVA, which is more appropriate given the experimental procedures were independent, as the reviewer pointed out.

> *The English language needs to be revised throughout the text.*

We have thoroughly revised the English language throughout the text.

> ***Reviewer #3 (Recommendations For The Authors):***
>
> *(1) Figure 3. Clarify the physiological importance of 100 μM ATP. Would the Herp rhythm warrant Ca2+ release rhythms under basal conditions? In 3J-K, the relatively weak effect of Herp knockdown on ITPR1/2 levels, albeit statistically significant, may not be physiologically significant. This calls into question the claimed Herp-ITPR axis that underlies the Ca2+ release phenotype. Further, the correlation certainly exists but further characterization of Herp KD cells would be required to address the mechanism.*

As previously reported, a broad range of ATP concentrations can induce Ca2+ activity in the astrocytes (Neary et al., 1988). Originally, we conducted an ATP dose-response analysis to observe ER Ca2+ release in our primary astrocyte culture. Our results show that ER Ca2+ release begins at 50 μM ATP and plateaus at 500 μM. Please refer to Author response image 3. We selected 100μM ATP for our experiments because it induces a medium level of ER Ca2+ response. Importantly, although measuring ATP concentrations at the synapse in vivo is challenging(Tan et al., 2017), estimates suggest synaptic ATP concentrations range from 5-500 μM (Pankratov et al., 2006). Thus, 100μM ATP is a physiologically relevant concentration that can affect nearby cells, including astrocytes, in the nervous system.

Author response image 3.

Cultured astrocytes were transfected with G-CEPIA1er ER and at 48hrs post transfection, cultured astrocytes were treated with various concentrations of ATP and Ca2+ imaging analysis was performed. (A) ΔF/F0 values over time following ATP application. (B) Area above curve values. Values in graphs are mean ± SEM (*p < 0.05, **p < 0.005, ***p < 0.0005, and ****p < 0.00005; one-way ANOVA).

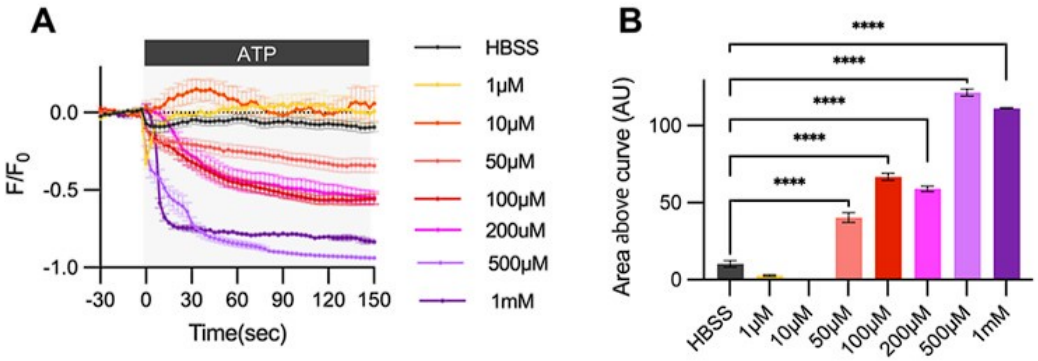

Regarding the comment on Ca2+ release rhythms under basal conditions, we interpret this as referring Ca2+ release in the absence of a stimulus. We typically observe Ca2+ release only upon stimulation, such as ATP treatment. However, we acknowledge that the modest effects of HERP knockdown on ITPR1/2 levels could question the HERP-ITPR axis's role in ER Ca2+ release.

To address this, we analyzed whether Herp KD induced increases in ER Ca2+ release were mediated through ITPRs by treating cells with Xestospongin C (XesC), an IP3R inhibitor. XesC treatment reduced ATP-induced ER Ca2+ release and eliminated the differences in ER Ca2+ release between control and Herp KD astrocytes (Fig. 3N – 3P). These results clearly indicate

that HERP-ITPR axis plays critical role in controlling ER Ca2+ release. These new experiments have been included in Fig. 3 and explained in the result section (lines 217-221).

Furthermore, following the reviewer's suggestion, we examined whether HERP rhythms underlie the rhythms of ER Ca2+ response by analyzing ER Ca2+ response in Herp KD astrocyte in two different times following synchronization. In control astrocytes, ATP-induced ER Ca2+ responses vary depending on time, whereas these time-dependent variations were abolished in Herp KD astrocytes. These new experiments have been included in Fig. 4K – 4M and explained in the Results section (lines 232-235).

Collectively, these results indicate that HERP rhythms lead to time-dependent differences in ER Ca2+ response through ITPRs.

> *(2) Figure 4K-L. As data suggested the involvement of ITPR1 and ITPR2 (circadian effect), a reasonable next step is to determine their involvement, but the study did not pursue the hypothesis.*

Thank you for your insightful comment. Our results indeed suggest that rhythms in ITPR2 levels may drive the time-dependent variations in ATP-induced ER Ca2+ release following synchronization. The newly conducted experiments demonstrated that treatment with the ITPR inhibitor XesC suppressed ATP-induced ER Ca2+ release at both control and Herp siRNA treatment conditions (Fig. 3). Based on these findings, we now further confirm that rhythms of ITPR levels, specifically ITPR2 underlie the circadian variations in ER Ca2+ release. While examining the effect of ITPR2 siRNA would directly prove the involvement of ITPR2, we have decided to pursue this experiment in the future studies.

> *(3) Figure 5A-C. Data from WT cells should be included side by side with Bmal1-/- cells for comparison which is expected to be consistent with the HERP levels as in 5D-E. Again, the role of ITPR2 is suggested but not demonstrated.*

Following the reviewer's suggestion, we conducted additional experiments including both WT and Bmal1-/- cultured astrocytes side-by-side. The results were consistent with our previous findings: WT astrocytes showed rhythms of ER Ca2+ release while Bmal1-/- astrocytes did not. We have updated the Figure 5A to 5C and the corresponding Results section in lines 242-245 accordingly.
Regarding second comment, as mentioned in our previous response, we plan to examine the role of ITPR2 in further studies.

> *(4) Figure 6. The Connexin data seems an addon and is correlative with the Ca2+ release. The role of Herp and Itpr in Connexin function is not addressed. Figure 6E-F was not called out in the results section. Suggest providing additional data to support the role of the HERP-ITPR axis in regulating Ca2+ release and Connexin activity.*

We agree that additional data are needed to support the role of HERP in regulating CX43 phosphorylation. Therefore, we have conducted further experiments to determine whether rhythms of Cx43 phosphorylation are regulated by HERP. In the control astrocytes, ATP treatment induced time-dependent variations in Cx43 phosphorylation. However, these rhythms were abolished in Herp KD astrocytes. These results indicate that rhythms in HERP levels contribute to the time-dependent variations in Cx43 phosphorylation. These new experiments have included in Fig. 6G and 6H and explained in the results section (lines 276-281).

Regarding second comment, we have corrected our oversight by properly referencing figures 6E-F in the results section. Please refer to lines 357-359 for clarification.

> *(5) Discussion. This section should focus on noteworthy points to discuss, not repeating the results.*

Based on the reviewer's valuable suggestions, we have revised the Discussion section to minimize repetition of the results. Thank you for your guidance.

> *(6) The manuscript exhibits numerous grammatical and textual inaccuracies that necessitate careful revision by the authors. My observations here are confined to the title and the abstract alone. I recommend altering the title from "mouse cultured astrocytes" to "cultured mouse astrocytes" for clarity and grammatical correctness. The abstract, meanwhile, needs enhancements both in terms of its content and language. It should incorporate the results of the partitioning among the ER, cytoplasm, and mitochondria, and provide clear definitions for some of the critical terms used. It's worth noting that the abstract's second sentence contains a grammatical error.*

Thank you for the reviewer's valuable feedback. We have carefully revised the title, abstract, and main text to address the grammatical and textual issues. The title has been changed to "cultured mouse astrocytes". Additionally, the abstract now includes results related to cytoplasmic Ca2+ dynamics and has been revised in several places. We appreciate your insights and have worked to enhance the content and language accordingly.

Reference

Agostinelli, F., Ceglia, N., Shahbaba, B., Sassone-Corsi, P., & Baldi, P. (2016). What time is it? Deep learning approaches for circadian rhythms. *Bioinformatics*, *32*(12), i8-i17. https://doi.org/10.1093/bioinformatics/btw243

Cahoy, J. D., Emery, B., Kaushal, A., Foo, L. C., Zamanian, J. L., Christopherson, K. S., Xing, Y., Lubischer, J. L., Krieg, P. A., Krupenko, S. A., Thompson, W. J., & Barres, B. A. (2008). A transcriptome database for astrocytes, neurons, and oligodendrocytes: a new resource for understanding brain development and function. *J Neurosci*, *28*(1), 264-278. https://doi.org/10.1523/JNEUROSCI.4178-07.2008

Carreras-Sureda, A., Pihán, P., & Hetz, C. (2018). Calcium signaling at the endoplasmic reticulum: fine-tuning stress responses. *Cell Calcium*, *70*, 24-31. https://doi.org/https://doi.org/10.1016/j.ceca.2017.08.004

Enkvist, M. O., & McCarthy, K. D. (1992). Activation of protein kinase C blocks astroglial gap junction communication and inhibits the spread of calcium waves. *J Neurochem*, *59*(2), 519-526. https://doi.org/10.1111/j.1471-4159.1992.tb09401.x

Fujii, Y., Maekawa, S., & Morita, M. (2017). Astrocyte calcium waves propagate proximally by gap junction and distally by extracellular diffusion of ATP released from volume-regulated anion channels. *Scientific Reports*, *7*(1), 13115. https://doi.org/10.1038/s41598-017-13243-0

Giorgi, C., Marchi, S., & Pinton, P. (2018). The machineries, regulation and cellular functions of mitochondrial calcium. *Nature Reviews Molecular Cell Biology*, *19*(11), 713-730. https://doi.org/10.1038/s41580-018-0052-8

Glynn, E. F., Chen, J., & Mushegian, A. R. (2006). Detecting periodic patterns in unevenly spaced gene expression time series using Lomb-Scargle periodograms. *Bioinformatics*, *22*(3), 310-316. https://doi.org/10.1093/bioinformatics/bti789

Hughes, M. E., Hogenesch, J. B., & Kornacker, K. (2010). JTK_CYCLE: an efficient nonparametric algorithm for detecting rhythmic components in genome-scale data sets. *J Biol Rhythms*, *25*(5), 372-380. https://doi.org/10.1177/0748730410379711

Ingiosi, A. M., Hayworth, C. R., Harvey, D. O., Singletary, K. G., Rempe, M. J., Wisor, J. P., & Frank, M. G. (2020). A Role for Astroglial Calcium in Mammalian Sleep and Sleep Regulation. *Curr Biol*, *30*(22), 4373-4383.e4377. https://doi.org/10.1016/j.cub.2020.08.052

Mei, W., Jiang, Z., Chen, Y., Chen, L., Sancar, A., & Jiang, Y. (2020). Genome-wide circadian rhythm detection methods: systematic evaluations and practical guidelines. *Briefings in Bioinformatics*, *22*(3). https://doi.org/10.1093/bib/bbaa135

Neary, J. T., van Breemen, C., Forster, E., Norenberg, L. O., & Norenberg, M. D. (1988). ATP stimulates calcium influx in primary astrocyte cultures. *Biochem Biophys Res Commun*, *157*(3), 1410-1416. https://doi.org/10.1016/s0006-291x(88)81032-5

Pankratov, Y., Lalo, U., Verkhratsky, A., & North, R. A. (2006). Vesicular release of ATP at central synapses. *Pflugers Arch*, *452*(5), 589-597. https://doi.org/10.1007/s00424-006-0061-x

Paredes, F., Parra, V., Torrealba, N., Navarro-Marquez, M., Gatica, D., Bravo-Sagua, R., Troncoso, R., Pennanen, C., Quiroga, C., Chiong, M., Caesar, C., Taylor, W. R., Molgó, J., San Martin, A., Jaimovich, E., & Lavandero, S. (2016). HERPUD1 protects against oxidative stress-induced apoptosis through downregulation of the inositol 1,4,5-trisphosphate receptor. *Free Radic Biol Med*, *90*, 206-218. https://doi.org/10.1016/j.freeradbiomed.2015.11.024

Szabó, Z., Héja, L., Szalay, G., Kékesi, O., Füredi, A., Szebényi, K., Dobolyi, Á., Orbán, T. I., Kolacsek, O., Tompa, T., Miskolczy, Z., Biczók, L., Rózsa, B., Sarkadi, B., & Kardos, J. (2017). Extensive astrocyte synchronization advances neuronal coupling in slow wave activity in vivo. *Scientific Reports*, *7*(1), 6018. https://doi.org/10.1038/s41598-017-06073-7

Tan, Z., Liu, Y., Xi, W., Lou, H. F., Zhu, L., Guo, Z., Mei, L., & Duan, S. (2017). Glia-derived ATP inversely regulates excitability of pyramidal and CCK-positive neurons. *Nat Commun*, *8*, 13772. https://doi.org/10.1038/ncomms13772

Torrealba, N., Navarro-Marquez, M., Garrido, V., Pedrozo, Z., Romero, D., Eura, Y., Villalobos, E., Roa, J. C., Chiong, M., Kokame, K., & Lavandero, S. (2017). Herpud1 negatively regulates pathological cardiac hypertrophy by inducing IP3 receptor degradation. *Sci Rep*, *7*(1), 13402. https://doi.org/10.1038/s41598-017-13797-z

Tsunematsu, T., Sakata, S., Sanagi, T., Tanaka, K. F., & Matsui, K. (2021). Region-specific and state-dependent astrocyte Ca^{2+} dynamics during the sleep-wake cycle in mice. *The Journal of Neuroscience*, JN-RM-2912-2920. https://doi.org/10.1523/jneurosci.2912-20.2021

Verkhratsky, A., & Nedergaard, M. (2018). Physiology of Astroglia. *Physiol Rev*, *98*(1), 239-389. https://doi.org/10.1152/physrev.00042.2016

Vyazovskiy, V. V., Olcese, U., Lazimy, Y. M., Faraguna, U., Esser, S. K., Williams, J. C., Cirelli, C., & Tononi, G. (2009). Cortical firing and sleep homeostasis. *Neuron*, *63*(6), 865-878. https://doi.org/10.1016/j.neuron.2009.08.024

Wu, G., Anafi, R. C., Hughes, M. E., Kornacker, K., & Hogenesch, J. B. (2016). MetaCycle: an integrated R package to evaluate periodicity in large scale data. *Bioinformatics*, *32*(21), 3351-3353. https://doi.org/10.1093/bioinformatics/btw405

Yang, R., & Su, Z. (2010). Analyzing circadian expression data by harmonic regression based on autoregressive spectral estimation. *Bioinformatics*, *26*(12), i168-174. https://doi.org/10.1093/bioinformatics/btq189

Yoo, S. H., Ko, C. H., Lowrey, P. L., Buhr, E. D., Song, E. J., Chang, S., Yoo, O. J., Yamazaki, S., Lee, C., & Takahashi, J. S. (2005). A noncanonical E-box enhancer drives mouse Period2 circadian

oscillations in vivo. *Proc Natl Acad Sci U S A*, *102*(7), 2608-2613. https://doi.org/10.1073/pnas.0409763102

https://doi.org/10.7554/eLife.96357.2.sa0